UNIVERSIDADE DE LISBOA
FACULDADE DE CIÊNCIAS
DEPARTAMENTO DE BIOLOGIA VEGETAL

Calcium Fluoride and Silver Nanocomposite Membranes for Biofouling Prevention

Luís Cláudio de Sousa

Mestrado em Microbiologia Aplicada

Dissertação orientada por:
Sílvia Patrícia Nunes Monteiro
Ana Maria Gomes Moura Pires de Andrade Tenreiro

2020

This Dissertation was fully performed at Instituto Superior Técnico under the direct co-supervision of Sílvia Patrícia Nunes Monteiro, Ana Sofia de Oliveira Figueiredo and Maria Norberta Neves Correira de Pinho.

Professor Ana Maria Gomes Moura Pires de Andrade Tenreiro was the internal supervisor designated in the scope of the Master in Applied Microbiology of the Faculty of Sciences of the University of Lisbon.

Agradecimentos

Em primeiro lugar gostaria de agradecer às minhas orientadoras. Às professoras Norberta Pinho e Ana Sofia Figueiredo, pela ajuda no estudo dos processos de membranas, e à doutora Sílvia Monteiro pelo acompanhamento constante e pelo apoio com os ensaios microbiológicos. Gostaria também de agradecer ao doutor Ricardo Santos, e aos restantes elementos do núcleo de Microbiologia – Novas Tecnologias do Laboratório de Análises do IST, ao Mário, à Adriana, à Daniela e à Mariana, pela ajuda ao longo desta dissertação.

Agradeço igualmente a toda a minha família, pelo seu apoio incondicional.

Resumo

A tecnologia de separação por membranas assume um papel cada vez mais importante no tratamento de águas. A permeação por membrana ocorre a partir de um gradiente de pressões entre a alimentação e o permeado, com a membrana a atuar como barreira à passagem de partículas ou solutos. A capacidade de separar componentes cada vez mais pequenos divide os processos de separação por membrana em quatro categorias: microfiltração (MF), ultrafiltração (UF), nanofiltração (NF) e osmose inversa (RO). As aplicações desta tecnologia são variadas, desde a dessalinização utilizando membranas de RO à remoção de agentes patogénicos de águas de consumo com membranas de UF. Ao longo do processo de permeação pode ocorrer a acumulação de componentes da alimentação na superfície da membrana e/ou dos poros (em membranas porosas como as de MF e de UF). Este fenómeno, designado por *fouling*, leva a uma diminuição do fluxo de permeado através da membrana, representando um dos maiores fatores limitantes à aplicação da tecnologia de membranas.

Dependendo do tipo de material acumulado na membrana, *fouling* pode ser dividido em quatro principais categorias: *fouling* coloidal, com a acumulação de partículas de elevadas dimensões; *fouling* inorgânico, como a precipitação de sais; *fouling* orgânico, com a adesão de diferentes compostos orgânicos ou polímeros; e *biofouling*, causado pela formação de biofilmes na superfície da membrana. São vários os processos usados no controlo de *fouling*, seja pelo pré-tratamento da alimentação ou pela utilização de ciclos de limpeza da membrana. No entanto, a eficácia de qualquer um destes processos é limitada. O pré-tratamento da alimentação é comum, mas comporta um aumento de custos e não previne completamente o aparecimento de *fouling*. A limpeza de membranas divide-se em dois grupos de processos: limpeza física e limpeza química. A limpeza física é utilizada em períodos regulares durante a operação de permeação, mas não permite uma recuperação completa da permeabilidade da membrana. A limpeza química é aplicada quando a perda de permeabilidade não é recuperável com limpeza física, sendo limitada pela possibilidade de causar degradação da membrana. *Biofouling* é particularmente problemático em termos de controlo. Para evitar a formação de biofilmes na membrana são necessários protocolos de desinfeção da alimentação; quando estes se revelam ineficazes, a remoção de biofilmes implica a limpeza química da membrana. Novas formas de controlo de *biofouling* são, portanto, necessárias. A modificação de membranas para a aquisição de resistência inata a *biofouling* é cada vez mais estudada. Estas modificações focam-se em diminuir a adesão dos biofilmes ou em diminuir a proliferação de células nos biofilmes. A segunda opção foi desenvolvida nesta dissertação. Membranas nanocompósitas – membranas com nanopartículas na matriz – foram desenvolvidas anteriormente, utilizando nanopartículas com conhecida, ou prevista, atividade antimicrobiana. Dois tipos distintos de membranas nanocompósitas de acetato de celulose para UF foram reproduzidas, a partir de trabalhos anteriores, e avaliadas em potencial antibacteriano como *proxy* para atividade anti-biofilme.

As membranas nanocompósitas de fluoreto de cálcio testadas nesta dissertação foram originalmente desenvolvidas por Estrada (Estrada, 2017). A atividade antibacteriana das membranas, ou das nanopartículas em si, não foi avaliada anteriormente. No entanto, esta atividade já foi observada com outras nanopartículas de fluoreto de cálcio (CaF_2 NP). A ação de CaF_2 NP é dependente da libertação do ião fluoreto para o meio. Já foram demonstradas várias interações entre F^- e o metabolismo de bactérias. F^-, sozinho ou em complexo com outros iões, inibe a atividade de enzimas como a enolase ou a ATPase. A homeostasia de pH das células é vista como um dos principais alvos de F^-. A entrada de F^- na célula é aumentada em meios com pH baixo: nestes ambientes, F^- tem tendência a formar ácido fluorídrico. A permeabilidade das membranas celulares a HF é superior a F^-, o que leva uma maior entrada na célula. No interior da célula, HF dissocia-se, simultaneamente diminuindo o pH intracelular e aumentando a concentração F^-, que por sua vez inibe a atividade de exportadores de protões.

Adicionalmente, a libertação de F^- de CaF_2 NP é aumentada em meios ácidos. A diminuição do pH aparenta ser um fator importante para aumentar a atividade destas nanopartículas.

A atividade antibacteriana de CaF_2 sob a forma de nanopartícula, e o impacto do pH nesta, não puderam ser avaliados nesta dissertação. Diversas variações do protocolo proposto por Estrada para a produção de CaF_2 NP falharam na produção de nanopartículas. O resultado da síntese foi, invariavelmente, a produção de partículas maiores que 100 nm, ou seja, de micropartículas. As micropartículas obtidas não mostraram efeito contra *Escherichia coli*, independentemente do pH do meio. A falta de atividade antibacteriana pode ser consequência do seu tamanho. Tendo em conta que as partículas descritas por Estrada não foram reproduzidas, e que as partículas produzidas não demonstraram atividade antibacteriana, as membranas nanocompósitas de fluoreto de cálcio não foram produzidas e testadas.

Prata, iónica ou sobre a forma de nanopartículas metálicas tem, ao contrário de CaF_2 NP, um historial alargado de aplicações em membranas. Nesta dissertação foram produzidas e testadas membranas de UF desenvolvidas por Figueiredo *et al.* (Figueiredo et al., 2015). A atividade antibacteriana destas membranas não foi estudada anteriormente. No entanto, as nanopartículas de prata (Ag NP) que incorporam já foram utilizadas na produção de outras membranas nanocompósitas de UF e NF, com efeito inibitório contra *E. coli*. Foram produzidos dois conjuntos de membranas de acetato de celulose, com diferentes teores de prata.

Apesar de serem geralmente reconhecidas como agentes antimicrobianos, o mecanismo de atividade das Ag NP é controverso. A atividade destas partículas é atribuída ou à libertação de iões de prata para o meio, ou a interações diretas das partículas com as células. Tal como as Ag NP, o ião Ag^+ é tido como um agente antimicrobiano eficaz. São vários os efeitos atribuídos a Ag^+; muitos deles comuns às Ag NP, como a formação de espécies reativas de oxigénio. O ião Ag^+ tem afinidade com grupos tiol de aminoácidos como a cisteína; ao ligar-se provoca modificações na conformação de proteínas, inativando-as. No entanto, alguns efeitos das Ag NP parecem ser exclusivos destas. Imagens de microscopia eletrónica de transmissão demonstram interações diretas de nanopartículas com componentes da célula, como a membrana e a parede celular, levando à sua desagregação, o que não se verifica com o ião Ag^+.

O mecanismo de ação das Ag NP não foi estudado nesta dissertação. No entanto, tem importância para o desenvolvimento de membranas nanocompósitas de prata. Nas membranas nanocompósita de prata, as nanopartículas encontram-se distribuídas em toda a matriz da membrana. Se uma interação direta entre a nanopartícula e a bactéria for necessária, apenas as partículas presentes na superfície da membrana estariam disponíveis para a inativação das bactérias. Por outro lado, um mecanismo dependente da libertação de Ag^+ seria mais sensível à composição da alimentação. O ião Ag^+ forma sais insolúveis com iões como Cl^- e S^{2-}, o que levaria a uma menor concentração de Ag^+ disponível em meios ricos nestes iões. A afinidade do ião Ag^+ com alguns aminoácidos leva a que em meios ricos nesses aminoácidos, ou proteínas que os contenham, a sua disponibilidade também diminua.

A adição das Ag NP às membranas de acetato de celulose levou ao aumento da sua permeabilidade hidráulica e à diminuição da sua seletividade a polímeros orgânicos. A atividade antibacteriana das membranas foi testada num conjunto de estirpes laboratoriais e de isolados ambientais de *E. coli*, *Enterococcus faecalis*, *Pseudomonas aeruginosa* e *Staphylococcus aureus*. A atividade antibacteriana das membranas variou entre bactérias e entre meios de cultura utilizados. *E. coli* WDCM 00013 sofreu uma inibição completa de crescimento num meio pobre em proteínas; num meio com maior abundância de proteínas não foi visível qualquer inibição. De todas as bactérias testadas, apenas *S. aureus* WDCM 00034 demonstrou sensibilidade às membranas nanocompósitas no meio mais rico em proteínas. A sensibilidade à prata não foi, portanto, constante entre as diferentes estirpes/isolados de

S. aureus. A atividade antimicrobiana das membranas é atribuível à libertação de prata pela membrana; no entanto, não foi determinado se a prata foi libertada sobre a forma de nanopartícula ou como ião. A sensibilidade à composição do meio é indicativa de que a atividade anti-biofilme destas membranas poderá estar dependente da composição da alimentação. Dada a pequena proporção de bactérias sensíveis às membranas encontrada durante esta dissertação, conclui-se que as membranas no seu estado atual não teriam atividade anti-biofilme, e que requerem mais desenvolvimento antes de uma futura aplicação.

Referências:

Estrada, A. M. (2017). *Efecto de la modificación de membranas asimétricas de acetato de celulosa con partículas ultrafinas de fluoruro de calcio*. Universidad Autónoma de San Luis Potosí.

Figueiredo, A. S., Sánchez-Loredo, M. G., Maurício, A., Pereira, M. F. C., Minhalma, M., & de Pinho, M. N. (2015). Tailoring of structures and permeation properties of asymmetric nanocomposite cellulose acetate/silver membranes. *Journal of Applied Polymer Science*, *132*(21). https://doi.org/10.1002/app.41796

Palavras-chave: *Biofouling*; Ultrafiltração; Membranas nanocompósitas; Nanopartículas de fluoreto de cálcio; Nanopartículas de prata.

Abstract

Membrane filtration systems are an increasingly important group of technologies in water treatment. The application of these technologies is severely limited by fouling. Fouling covers a large group of phenomena in which the membrane surface and/or pores are blocked by the deposition of materials from the feed, leading to a decrease in the permeability of the membrane. Biofouling – formation of biofilms on the surface of a membrane – can be troublesome, as it is hard to prevent and treat. Previous works have created novel membranes, aiming at preventing biofouling. A particular subset of these are nanocomposite membranes, membranes containing nanoparticles with an anti-biofouling potential. In this dissertation, two previously developed nanocomposite membranes were produced and tested for antibacterial activity, as a proxy for anti-biofouling activity. Calcium fluoride nanocomposite membranes were yet to be tested for antibacterial activity. The nanoparticles they contained were also untested. Fluoride, released by CaF_2 nanoparticles, is known to affect bacteria, in a pH-dependent mechanism. The protocol used for the synthesis of the CaF_2 particles failed to produce nanoparticles, even after several variations were made. The resulting microparticles lacked antibacterial action against *Escherichia coli* under acidic and neutral media, most likely due to their large size. As the particles were not the intended size and lacked activity, the nanocomposite membranes were not produced and tested. Silver nanocomposite membranes, on the other hand, have shown antibacterial potential in previous works. Asymmetrical cellulose acetate ultrafiltration membranes with different silver contents were characterized on hydraulic properties and tested against laboratory strains and environmental isolates of *E. coli*, *Enterococcus faecalis*, *Pseudomonas aeruginosa* and *Staphylococcus aureus*. Nanocomposite membranes showed increased hydraulic permeabilities at the cost of lower selectivity. The activity of the membranes varied among bacteria and was dependent on the composition of the growth media. *E. coli* growth was completely inhibited in a protein poor medium but was almost unaffected in a protein rich medium. Of all the tested bacteria, only *S. aureus* WDCM 00034 was inhibited in the protein rich medium. Further development is necessary on silver nanocomposite membranes before application in filtration systems.

Keywords: Biofouling; Ultrafiltration; Nanocomposite membranes; Calcium fluoride nanoparticles; Silver nanoparticles.

Content

List of Figures and Tables

Abbreviations

Ag NP – Silver nanoparticle

CaF_2 MP – Calcium fluoride microparticle

CaF_2 NP – Calcium fluoride nanoparticle

Cfu – Colony forming unit

DLS – Dynamic light scattering

EPS – Extracellular polymeric substances

f – Rejection coefficient

J_p – Permeate flux

MBR – Membrane bioreactor

MF – Microfiltration

MRD – Maximum recovery diluent

MRSA – Methicillin-resistant *Staphylococcus aureus*

MWCO – Molecular weight cut-off

NF – Nanofiltration

OD – Optical density

PEG – Polyethylene glycol

PVP – Polyvinylpyrrolidone

Q_f – Feed mass flow rate

RO – Reverse osmosis

SDW – Sterile de-ionized water

TBX – Tryptone bile x-glucuronide

TMP – Transmembrane pressure

TOC – Total organic carbon

TSA – Trypticase soy agar

TSB – Tryptic soy broth

UF – Ultrafiltration

UV – Ultraviolet

1. Introduction

Water scarcity is one of the most pressing issues Humanity faces. Access to safe drinking water is compromised across the globe, due to water pollution and scarcity of viable water sources (Saurí, 2013). Simultaneously, many of the water sources available are explored to unsustainable levels (Lall et al., 2020). The use of seawater or reuse of wastewater or greywater can help to overcome the required needs for water. Membrane separation technologies, first developed in 20th century, have become a reliable option to treat these waters. However, the application of membrane technologies is limited by the multifaceted problem of fouling. Fouling decreases the productivity of the membrane systems, greatly increasing the costs of operation. For a broader application of membrane filtration systems to treat water, the issues with fouling have to be overcome.

1.1. Membrane separation technologies

Membrane permeation is a pressure driven process. Membrane systems are operated either in dead-end or crossflow filtration (figure 1.2) (Crittenden et al., 2012; Koros et al., 1996). In dead-end filtration, the solution to be filtered – feed – moves perpendicularly to the membrane surface; retained particles/solutes – retentate – remain on the membrane surface. In crossflow filtration, the feed moves in parallel to the membrane; the permeate side of the membrane is kept at a lower pressure, forcing part of the feed to pass through the membrane; as solvent and non-retained particles/solutes are removed from the feed, its constitution changes, becoming a concentrate stream that is continuously removed.

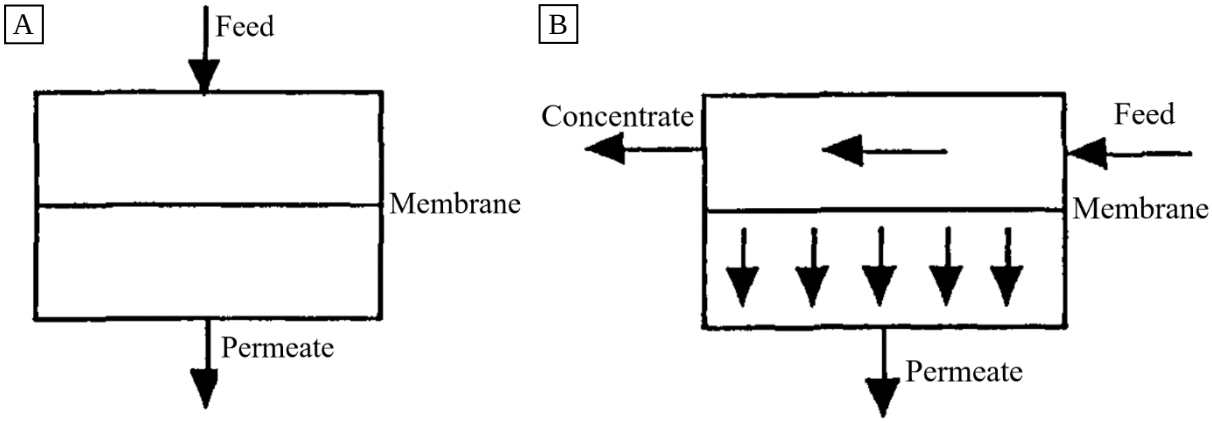

Figure 1.1– A) Dead-end filtration system; B) Crossflow filtration system. Adapted from Koros *et al.* (Koros et al., 1996).

Pressure-driven membrane processes are divided into four categories, based on the ability to separate increasingly smaller particles and solutes: microfiltration (MF), ultrafiltration (UF), nanofiltration (NF) and reverse osmosis (RO) (figure 1.1). MF and UF membranes can be further classified as porous membranes, and RO membranes as non-porous membranes; NF membranes are variably reported as porous and non-porous membranes (Allgeier et al., 2005; Crittenden et al., 2012; Landsman et al., 2020). The separation mechanism between the two groups is substantially different. Each MF/UF membrane has a characteristic distribution of pore sizes (Allgeier et al., 2005). MF and UF membranes separate feed components by sieving, with particles larger than the membrane's largest pores being completely retained (Allgeier et al., 2005). MF membranes remove suspended particles, including bacteria, and large colloids. UF membranes retain virus and large macromolecules like proteins and polysaccharides. NF and RO separation mechanism is based in a solution/diffusion model of solutes through the membrane, by the process of reverse osmosis (Allgeier et al., 2005; Crittenden et al., 2012): a pressure above the osmotic pressure of the system is exerted, forcing the solvent to pass through the semipermeable membrane. NF and RO membranes retain most organic and inorganic

solutes, with NF's decreased capability of removing monovalent ions from solution differentiating both membranes (Landsman et al., 2020).

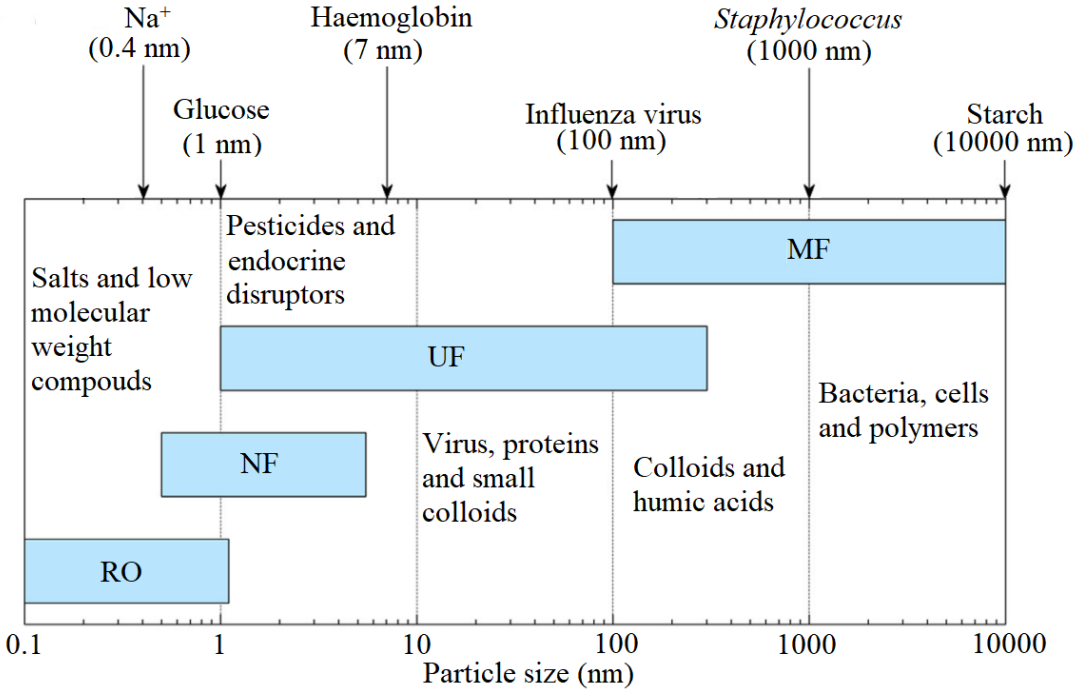

Figure 1.2 – Schematical representation of the size exclusion capabilities of membrane filtration systems; Adapted from Madsen (Madsen, 2014).

Membrane systems have multiple uses in water treatment, both in the production of drinking water and in wastewater treatment. RO systems are applied in seawater and brackish water desalination, offering lower energy costs than common distillation methods (Semiat, 2008). RO can also be used for wastewater reuse, for the production of water for irrigation, for example (Plappally & Lienhard V, 2012). The retention of divalent ions by NF membranes, combined with lower pressure requirements compared with RO membranes, makes NF a valuable option for decreasing water hardness (Allgeier et al., 2005). NF is also applied in drinking water treatment, where/when the removal of large amounts of organic carbon is required (Madsen, 2014). MF and UF are both applied to drinking water treatment in combination with other treatments, to efficiently remove microbial contamination (Crittenden et al., 2012). MF and UF are also used in wastewater treatment: membrane bioreactors (MBR) combine the biological degradation of waste common in wastewater treatments with membrane filtration, decreasing the size of the wastewater treatment plants and increasing the quality of the effluent (Miura et al., 2007).

In filtration systems, membranes are organized into membrane modules (Crittenden et al., 2012) with various existing types, including hollow fiber membranes and spiral-wound membranes. Hollow fiber membranes are composed by bundles of thin tubes (0.5 mm to 2 mm diameter), resulting in a large membrane surface; depending on the installation, the feed can travel either inside or outside the fiber (Allgeier et al., 2005). In spiral-wound membranes, several sheets of membrane surround a central permeate collection tube; membrane sheets are organized in sets of two, separated by spacers, with a permeate collection space between them, and a feed/concentrate stream on the outside (Crittenden et al., 2012). During the stages of development and testing, the membranes can also be used as a singular flat membrane sheet, placed inside a membrane cell (Petersen, 1993).

Organic polymers are the most common type of membrane material (Ng et al., 2013). Depending on the polymer and production method, the membranes can have different morphologies (Fane et al.,

2015). Symmetrical membranes have a uniform structure; other membranes types, namely composite and asymmetrical membranes, have different morphologies between their feed and permeate sides. This can be advantageous, as it allows for a thinner, more selective, surface and a thicker support with smaller hydraulic resistance (Petersen, 1993). Composite membranes are produced by depositing a polymer layer on top of a pre-produced support of another material(Petersen, 1993). Alternatively, a single membrane material can be used, as is the case with asymmetrical cellulose acetate membranes produced by the wet-phase inversion process, as described by Kunst and Sourirajan (Kunst & Sourirajan, 1974). In the wet-phase inversion process, a solution composed by a solvent, a non-solvent and cellulose acetate – designated by casting solution – is spread evenly over a flat surface and briefly exposed to air. The solvent from the exposed face evaporate at a fast rate, leading to the precipitation of the polymer, creating a thin but dense layer – the active layer – responsible for the separation characteristics of the membrane (Kesting & Menefee, 1969). The membrane is then placed in a coagulation bath (a cold-water bath). The formation of the active layer and pore in cellulose acetate asymmetrical membranes was first explained by Kesting and Menefee (Kesting & Menefee, 1969), using acetone as the solvent and formamide as the non-solvent. The formation of the pore is the result of the larger solubility of cellulose acetate in the mixture of acetone/formamide compared to formamide alone. When both solvents are present, the polymer remains dissociated and in solution. As acetone progressively leaves the casting solution in the coagulation bath, the polymer precipitates, leaving circular droplets of formamide evenly dispersed in the membrane. Since the droplets contain low volumes of cellulose acetate, as the membrane solidifies voids are left in their place; the intersection of these voids subsequently leads to the development of a continuous network of pores. The droplet size increases with the increase in the initial ratio of formamide in the casting solution. Consequently, these membranes can be very dense on low formamide casting solutions, or more porous when a larger proportion of formamide is present in the casting solution.

1.2. Fouling

Despite the advantages of membrane systems over other technologies, their application remains limited by fouling, a process common in these systems (Guo et al., 2012). Fouling is caused by the accumulation or adsorption of material on the surface of the membrane and on the membrane pores (in MF and UF); as material accumulates on the membrane, the hydraulic resistance increases, resulting in the decrease in the permeate flux (Ng et al., 2013; Shi et al., 2014). Membrane fouling can be divided into four categories, depending on the nature of the material accumulated on the membrane surface (Al-Amoudi & Lovitt, 2007; Shi et al., 2014): colloidal fouling/cake formation, inorganic fouling, organic fouling, and biofouling (Guo et al., 2012). Membrane cake occurs when large particulate or colloidal matter physically blocks the membrane surface or pores; inorganic fouling, or scaling, is composed by inorganic material, such as precipitated salts; organic fouling results from the binding of different organic compounds to the membrane surface; biofouling is usually defined as the development of biofilms on the membrane surface. Membrane systems can be operated at either a constant transmembrane pressure (TMP), or at a constant permeation flux (Guo et al., 2012). Therefore, as fouling develops, the yield of the filtration process decreases in systems running at a constant TMP, or the TMP must be increased if a target permeation flux is to be achieved.

The exact nature of biofouling is disputed, with overlap on the definitions of organic fouling and biofouling. Extracellular polymeric substances (EPS) sometimes fall on the category of organic foulants (Al-Amoudi & Lovitt, 2007), despite being essential elements of a biofilm. The development of a membrane biofilm (figure 1.3) starts with the formation of a conditioning film, composed by a variety of organic compounds and biologic polymers present in the feed, followed by the adhesion of bacteria to the membrane surface (Matin et al., 2011). The adhered microorganisms then proliferate and produce EPS, forming a mature biofilm, from which bacteria may release and colonize new surfaces

(Matin et al., 2011). Conditioning films also act as foulants (Bar-Zeev et al., 2015). Some differences are expected in the mechanism behind biofouling formation, depending on the characteristics of the feed. Transparent exopolymer particles, polymers common in marine water and responsible for the formation of the conditioning film in salt-water RO (Bar-Zeev et al., 2015) will not be present in groundwater used as feed in UF, for example. Bar-Zeev *et al*. proposed that pre-formed biofilms (protobiofilms) present in salt water feed for RO speeded up biofouling formation (Bar-Zeev et al., 2012). This difference in feed composition extends to the bacterial diversity expected in the biofilm. Membrane biofilms are composed by different communities of bacteria, and potentially by other microorganisms such as fungi (Baker & Dudley, 1998). Khan *et al.* and Inaba *et al* found substantially different bacterial communities in fouled saltwater RO membranes and in UF membranes used in MBR, respectively (Inaba et al., 2017; Khan et al., 2013). Bacterial communities also vary depending on the severity of fouling and on their location on the membrane module (Nagaraj et al., 2017). The concept of ecological succession can be applied, to some extent, in biofouling: Bereschenko *et al* observed that bacteria from the genus *Sphingomonas* were responsible for the initial colonization of a RO membrane, developing a biofilm that acted as a conditioning film for other bacteria (Bereschenko et al., 2010). No defined bacterial communities can therefore be predicted across all membrane biofilms. Overall, biofouling cannot be approached as a single problem, with a single cause and therefore a single solution across all membrane filtration systems.

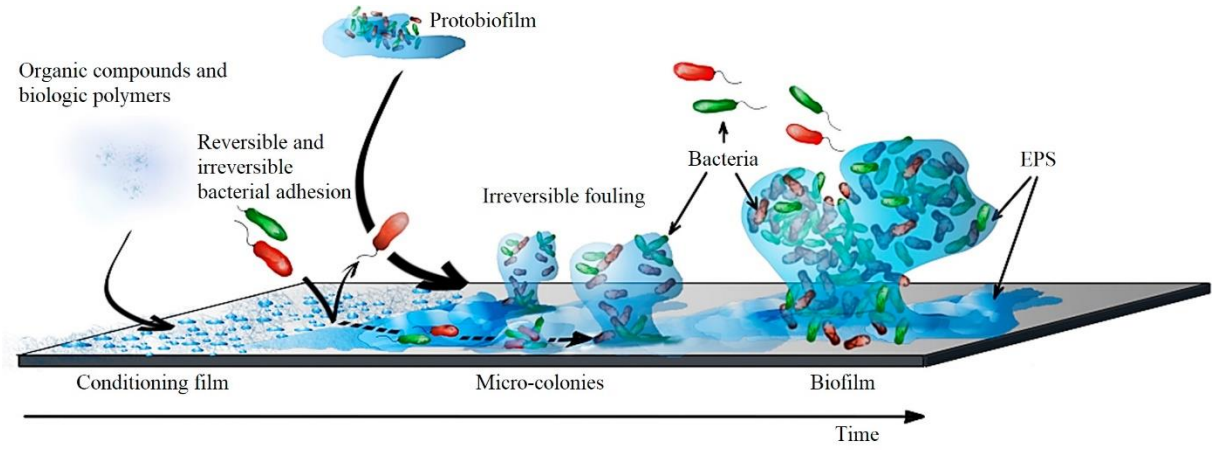

Figure 1.3 – Schematical representation of the formation of membrane biofilms. Adapted from Bogler *et al.* (Bogler et al., 2017).

In addition to feed composition, other factors affect the formation of fouling, namely the membrane module type, operation characteristics, and membrane surface characteristics. The different types of membrane modules have specificities in terms of fouling. For example, a spiral-woven membrane module is affected by fouling both on the membrane surface and in the membrane spacers (Tran et al., 2007). Hollow fiber modules can suffer from blockages that completely stop the flow of feed inside the fiber (Mickols, 2012). Dead-end filtration systems are more susceptible to cake formation, as all retained components of the feed are kept on the membrane surface during filtration. In comparison, crossflow filtration results in a tangential flow that continuously removes foulants from the membrane surface; an increase in the flow velocity has been shown to decrease the amount of cake formation (McCarthy et al., 2002). As surface adhesion of foulants is mediated by non-covalent interactions, the chemical and physical characteristics of the surface will have a large impact on the type and amount of fouling. Rougher membranes tend to be more susceptible to biofouling (Mansouri et al., 2010). Hydrophilic and hydrophobic membrane surfaces have both been reported as more susceptible to biofouling depending on the microorganism (Mansouri et al., 2010). However, hydrophilic surfaces are still seen as preferable, as they are more resistant to organic fouling (Kochkodan & Hilal, 2015).

Fouling can be controlled in two major steps: pretreatment of the feed and membrane cleaning. Feed pretreatment can be accomplished with various possible physical and chemical processes. For example, the feed water from industrial RO plants is commonly subjected to sedimentation and filtration; UF and MF membranes have both been used for this purpose (Badruzzaman et al., 2019). Coagulants (compounds that lead to the coagulation of previously dissolved organic compounds) and adsorbents (particles that due to surface characteristics accumulate organic foulants) are used in MF and UF pretreatment, both causing an increase in the overall size of the foulant (Huang et al., 2009). This approach results in the improvement of the filtration process in two ways: the filtration can become more selective, as previously small and permeable compounds become large enough to be retained in the membrane, and organic foulants are converted to membrane cake, which is easier to remove (Huang et al., 2009). Water disinfection is used to prevent biofouling (Gao et al., 2011). However, this is frequently ineffective or counterproductive. Chlorination has been found to increase the amount of carbon available for bacterial metabolism present in water (Polanska et al., 2005). As a complete sterilization of the feed would be required to avoid biofilm formation on the membrane surface (Mansouri et al., 2010), biological control of feed is unlikely to lead to complete biofouling prevention. Additionally, any form of pretreatment implicates an increase in size and energy/monetary cost of the installation (Zhang et al., 2016). The maximum permeate flux of a membrane is achieved when the membrane is new. The permeate flux gradually decreases due to fouling with continuing filtration. Several physical and chemical cleaning procedures are used to recover part of the initial permeate flux (Gao et al., 2011). Membrane backwashing, a physical cleaning process, is the most common form of membrane cleaning and is applicable to both dead-end and crossflow filtration (Cogan et al., 2016; Shi et al., 2014). In this process, permeate or clean water is forced to pass through the membrane from the permeate side, leading to the detachment of foulants (Shi et al., 2014). Backwashing is usually done periodically during membrane operation (Decarolis et al., 2001). Physical cleaning methods are limited in their cleaning capability (Yamamura et al., 2007). Their success, or lack thereof, leads to two categories of fouling: reversible and irreversible fouling (Kimura et al., 2004). When irreversible fouling is too large for efficient operation, chemical cleaning is applied (Cogan et al., 2016). The use of chemical cleaning is limited to extreme cases of fouling, as it can damage the membranes (Yamamura et al., 2007) while increasing the operation costs. The choice of pretreatment and cleaning protocols is limited by the membrane materials. Cellulose acetate membranes, for example, are degraded at low pH (H. B. Park et al., 2008), impairing the use of more acidic cleaning solutions (Shi et al., 2014).

Membrane biofilms routinely develop into irreversible fouling (Cogan et al., 2016). Given the limitations of the previously described processes, research as focused on modifying membranes to obtain an innate resistance to biofouling.

1.3. Membrane modifications

Most membrane modifications for biofouling prevention have focused on one of two issues – bacterial adhesion and bacterial growth (Mansouri et al., 2010). Prevention of bacterial adhesion is achieved by modifying the surface characteristics of the membrane, which can include surface charge, hydrophilicity and roughness, by various means (Kochkodan & Hilal, 2015): multiple polymers may be mixed to obtain new membranes with a less susceptible surface; the surface of the membrane can be coated with additives or grafted with *in situ* polymerization of brush-like structures (Mansouri et al., 2010). These solutions aim at reducing both EPS and bacterial adhesion or at facilitating their removal (Mansouri et al., 2010).

In contrast, solutions based on the control of bacterial growth seek to decrease biofilm proliferation. In this context, the entire membrane matrix (Sprick et al., 2018) or just the surface of the membrane may be modified, allowing, in this case, for post-production modification (Cruz et al., 2015).

Nanocomposite membranes, for example, contain nanoparticles with potential antibacterial activity in the matrix. The presence of antibacterial nanoparticles can give the membrane anti-biofouling properties, and simultaneously change the hydraulic properties of the membrane (Figueiredo et al., 2015). Various nanomaterials have been tested for this purpose (Esfahani et al., 2019) – halloysite nanotubes decorated with copper nanoparticles, for example, reduced the growth of bacteria when applied to UF membranes (Duan et al., 2015). Two different nanoparticles were studied in this dissertation – calcium fluoride nanoparticles (CaF_2 NP) and silver nanoparticles (Ag NP). Both are based on established antibacterial principles and used in the production of nanocomposite asymmetrical cellulose acetate ultrafiltration membranes.

1.3.1. Calcium fluoride nanoparticles: Most applications of calcium fluoride to date have focused on dentistry. Fluoride became of interest when regions with water supplies rich in the ion were found to have smaller incidences of tooth decay (Harrison, 2005). Since then, F^- compounds have been added to water and to some consumer products to replicate this effect (Bratthall et al., 1996). The anticariogenic activity of F^- has been linked to effects on the structure of the teeth and to antibacterial activity (Buzalaf et al., 2011). Given the biofilm-related origin of cariogenic lesions (Buzalaf et al., 2011), fluoride-releasing compounds may be useful in controlling biofouling.

The interactions of F^- with bacteria have been previously studied, frequently focusing on cariogenic bacteria like *Streptococcus mutans* (Liao et al., 2017). F^- acts by inhibiting several enzymes, both *in vitro* and *in vivo* (Liao et al., 2017), although this action is frequently dependent on the formation of other fluorine-containing ions (Marquis et al., 2003). In *S. mutans*, F^- inhibits multiple cell functions, like glycolysis and pH homeostasis. The former has been linked to an inhibition of the enzyme enolase (responsible for the conversion of 2-phosphoglycerate to phosphoenolpyruvate during glycolysis)(Curran et al., 1994). A decrease in acid tolerance of *S. mutans* by F^- is known to occur through various mechanisms (Marquis, 1990). F-ATPase (while acting as an ATP-dependent proton exporter) is inhibited by fluoride-aluminum ions (Sturr & Marquis, 1990). F^- intake by the cell increases with the decrease of external pH (Whitford et al., 1977), due to the high permeability of hydrogen fluoride (HF) compared to F^- (Gutknecht & Walter, 1981). HF forms in acidic external environments containing F^- (Ji et al., 2014). HF then permeates through the cell membrane. In the near neutral interior of the cell HF dissociates, simultaneously decreasing the internal pH and increasing the concentration of F^- (Marquis et al., 2003). Therefore, the presence of F^- in the medium deregulates the pH homeostasis of bacteria by simultaneously acting as a proton transporter and inhibiting proton extrusion by the cell (Marquis et al., 2003).

The antibacterial action of CaF_2 NP is the result of F^- release (Kulshrestha et al., 2016). CaF_2 NP have been shown to have antibiofilm activity against *S. mutans* without causing cell death (Kulshrestha et al., 2016). Bala *et al.* (Bala et al., 2017), however, obtained bactericidal activity against *Escherichia coli*, *Pseudomonas aeruginosa*, *Bacillus badius* and *Staphylococcus aureus*. The comparison between the two studies is difficult as the first study used much larger doses of smaller particles than the second work. Additionally, the second study also tested micrometer-ranged particles, and detected no activity. This highlights two important issues: whether sensitivity to F^- is sufficiently common in bacteria for other applications such as in membranes; and the importance of particle characteristics, including particle size, on the release of F^-. F^- release from CaF_2 NP contained in dental fillers has been shown to increase with the decrease in pH (H. H. K. Xu et al., 2010). This information suggests that acidic environments may, therefore, increase the antibacterial activity of CaF_2 NP, by simultaneously increasing the release and the activity of F^-.

CaF_2 NP nanocomposite membranes are a novel and untested solution in biofouling prevention. These membranes were first produced by Estrada (Estrada, 2017) although neither the antibacterial action of the particles nor of the membranes was evaluated.

1.3.2. Silver nanoparticles: Metallic silver and silver compounds have a long history of use as a form of microbiological control. Silver utensils and coins were once used to avoid spoilage of water and milk (Medici et al., 2019), and during the 19th and early 20th century (before the discovery of antibiotics) silver salts were used in the treatment of burns and ulcers, preceding any knowledge of the actual antibacterial activity of silver (Klasen, 2000b). The development of antibiotics reduced the interest in silver salts in medicine, although certain applications remained: silver sulphadiazine was still used as a topical antibacterial in burns at the end of the 20th century (Klasen, 2000a), although this use has since been disputed (Wasiak et al., 2013). Similarly, Ag NP have been studied and used for over 100 years (Nowack et al., 2011). For most of this time they were reported only as silver containing products or colloidal silver (Nowack et al., 2011) and not as nanoparticles. This may lead to the impression that "silver nanoparticles" are recent materials, which is not true. Early uses of these particles already took advantage of Ag NP's antibacterial activity (Nowack et al., 2011). Ag NP are currently present in a wide variety of materials and products, including fabrics, plastics, and bandages (Chernousova & Epple, 2013).

Despite their well-established antibacterial activity, the mechanism of action of Ag NP is still controversial. The debate is centered on the existence of particle-specific interaction between Ag NP and the cell (Xiu et al., 2012). In its absence, Ag NP's antibacterial activity is explained by the release of silver ions (Ag^+) by particle oxidation (Xiu et al., 2012), with a mechanism of action comparable to ionic compounds like silver nitrate.

Multiple mechanisms have been proposed for the antibacterial activity of Ag^+. Ag^+ are known to bind to various amino acids and subsequently to peptides and proteins (Eckhardt et al., 2013). The binding to proteins disrupts the structure and functions of the proteins, resulting in various physiological effects (Gordon et al., 2010). Thiol containing molecules possess a strong affinity to Ag^+ (Liau et al., 1997): amino acids like cysteine are known to bind to free Ag^+ when added to a growth medium, inactivating the antibacterial activity of Ag^+ (Liau et al., 1997). Additionally, Ag^+ has been reported to interact and as a result condense DNA in bacteria (Feng et al., 2000). This multitude of interactions renders impossible the definition of a single mechanism behind cell death attributable to Ag^+. Instead, several physiological effects have been observed, including some common to Ag NP. Modifications to the electron transport chain have reported for both, for example (Gordon et al., 2010; Li et al., 2010), as have the formation of reactive oxygen species (H.-J. Park et al., 2008; Quinteros et al., 2016) or the loss of proton motive force (Holt & Bard, 2005; Lok et al., 2007). Like Ag^+, the activity of Ag NP in nanocomposite ultrafiltration membranes has been suppressed by addition of cysteine (Zodrow et al., 2009). Lok *et al* observed that bacteria resistant to Ag^+ (as a $AgNO_3$ solution) were also resistant to Ag NP (Lok et al., 2007). Additionally, Ag NP produced and kept under anaerobic conditions, stopping any possible particle oxidation and Ag^+ release, lacked antibacterial activity (Xiu et al., 2011). Given that Ag NP surface oxidation is a widely accepted phenomenon, these observations lead to the conclusion that silver ion release must, at least, contribute to the antibacterial activity of Ag NP (Eckhardt et al., 2013).

Other works, however, have suggested a more direct action of the nanoparticle. Transmission electron microscopy images of Ag NP interacting with bacteria have been obtained previously, displaying substantially different effects between Ag^+ and Ag NP. Ag^+ treated *E. coli* cells displayed detached cell membranes and condensed DNA (Feng et al., 2000), phenomena not observed in Ag NP treated cells (Sondi & Salopek-Sondi, 2004). The latter treatment led to cell wall and membrane

degradation. The cell wall and membrane are frequently indicated as a major site of interaction with Ag NP. Similarly to *E. coli*, the cell wall of a Gram positive bacteria (*S. aureus*) presented damage as a result of interaction with Ag NP (Mirzajani et al., 2011). The previously discussed physiological effects, common to Ag^+ and Ag NP treated cells, have also been attributed to modifications in membrane permeability (Marambio-Jones & Hoek, 2010) and direct interaction with enzymes (Li et al., 2010) by Ag NP. Ag NP have also been observed inside cells (Morones et al., 2005; X.-H. N. Xu et al., 2004), which has resulted in multiple hypothesis. A "Trojan horse" effect has been suggested, with Ag NP penetrating the cell and releasing Ag^+ in the interior (Panáček et al., 2006). Direct interactions between the particle and different proteins, or molecules like DNA, inside the cell has also been proposed (Morones et al., 2005).

The wide variety of different, and frequently incompatible, explanations do not necessarily implicate any as false. "Silver nanoparticle" encompasses a large group of particles, with different sizes, shapes and surface characteristics (like stabilization or charge), all of which have been proposed as affecting the antibacterial activity of the particles (Choi & Hu, 2008; El Badawy et al., 2011; Helmlinger et al., 2016). As such, it is possible that different particles display different antibacterial mechanisms.

Although outside the scope of this dissertation, the mechanism of action is still an important consideration for the production of silver nanocomposite membranes. If contact between the nanoparticle and the bacterium is necessary, only Ag NP present on the feed side of the membrane may act as an anti-biofoulant, and considering the concurrent formation of biofouling and organic fouling, the antibacterial activity would quickly disappear. Antibacterial activity based on a diffusible agent, like Ag^+, could also present challenges. For instance, ultrafiltration membranes are permeable to salts, which may result on the leaching of the agent away from the membrane surface and into the permeate stream during filtration, as showed for polysulfone–silver nanocomposite membranes by Taurozzi *et al.* (Taurozzi et al., 2008). Ag^+ release-based membranes would also be more susceptible to feed composition. Ag^+ can form various insoluble salts with most halide ions – Cl^-, Br^- and I^- – and with S^{-2}, for example, with subsequent decrease in availability (Gupta et al., 1998). This interaction may be concentration dependent – Gupta *et al.* (Gupta et al., 1998) showed an increase in the antibacterial activity of a silver nitrate solution against *E. coli* when subjected to higher concentrations of NaBr or NaCl. This increase in activity was attributed to the formation of soluble silver/halide anions like $AgCl_2^-$ or $AgCl_3^{-2}$ that occurred at larger halide concentrations; at lower concentrations, silver halide salt formation would be more significant, reducing the amount of silver in solution. As previously discussed, Ag^+ can also bond to extracellular organic compounds, leading to inactivation.

Given the widely recognized antibacterial activity, several previous works have developed and tested silver nanocomposite membranes. Studies have been made with various membrane types and materials, nanoparticle characteristics and locations in the membrane (Mansouri et al., 2010). In this dissertation, asymmetrical ultrafiltration cellulose acetate membranes previously developed by Figueiredo *et al* (Figueiredo et al., 2015) were reproduced and tested for antibacterial activity with two silver contents in the casting solution: 0.14 % and 0.4 % . These membranes have yet to be tested for antibacterial activity. However, ultrafiltration (Figueiredo, 2016) and nanofiltration (Beisl et al., 2019) membranes with similarly produced silver nanoparticles have displayed such activity against *E. coli*.

1.4. Work overview

With the aim of preventing biofouling, several modified ultrafiltration membranes have been previously produced. Two different nanocomposite membranes – membranes modified by inclusion of nanoparticles in the membrane matrix – were reproduced and tested with this objective. Membrane anti-biofouling potential was evaluated by testing the nanoparticles/membranes for antibacterial activity. CaF_2 NP, as synthetized by Estrada (Estrada, 2017), have yet to be tested. Given that different

nanoparticles of the same chemical composition can have different activities, as previously discussed, these nanoparticles were tested for antibacterial activity against *E. coli* before being applied in membranes. In contrast, the membranes produced by Figueiredo *et al* (Figueiredo et al., 2015) use Ag NP with previously established activity against *E. coli* (Beisl et al., 2019). Thus, a set of two previously untested membranes, with different Ag NP contents, was produced and examined for antibacterial activity. As already discussed, no defined communities are expected in membrane biofilms. As such, a variety of both Gram-positive and Gram-negative bacteria were used when testing the antibacterial activity of the nanoparticles/membranes. Resistance to silver can vary between strains of the same species (Gupta et al., 1998). Since silver can be found in water sources (Ratte, 1999), the possibility of environmental bacteria obtaining resistance to these agents cannot be excluded. As such, laboratory strains and environmental isolates of *E. coli*, *Enterococcus*, *S. aureus* and *P. aeruginosa* were tested.

2. Materials and Methods

2.1. Bacterial strains/isolates

The laboratory strains *Enterococcus faecalis* WDCM 00009, *S. aureus* WDCM 00034 and *P. aeruginosa* WDCM 000024 were obtained from Eurofins Hydrologie (Douai, France); *E. coli* WDCM 00013 was obtained from ielab Calidad (Alicante, Spain). Environmental isolates of these bacteria were obtained from a variety of water sources (table 2.1).

Table 2.1- Water sample sources.

Sample	Description
A	Wastewater treatment plant effluent
B	Untreated wastewater
C	Wastewater treatment plant effluent
D	Untreated wastewater
E	Wastewater treatment plant effluent
F	Pool water
G	Spa resort water (before use)
H	Human consumption water
I	Spa resort water (before use)

E. coli and *Enterococcus* were isolated from both treated and untreated wastewaters – samples A, B, C, D and E. For both fecal bacteria, a single isolate for each species/genus was obtained from each water sample. *S. aureus* was isolated from sample F. Three isolates were obtained from this sample. Additionally, a previously isolated methicillin-resistant *S. aureus* (MRSA) was also tested. *P. aeruginosa* was isolated from samples G, H, and I. Two isolates were obtained from samples G and H; a single isolate was obtained from sample I. Throughout this dissertation, each isolate is identified by the presumptive species/genus, the letter corresponding to the sample from which it was isolated, and for *S. aureus* and *P. aeruginosa* a number differentiating the multiple isolates from each sample. Environmental isolates were obtained with the following methodology.

- *E. coli*: wastewater samples were kept at 5 ºC ± 3 ºC from recovery until used. Each wastewater sample was diluted with sterile de-ionized water (SDW) before being filtered with a 0.45 µm pore filter (Whatman). The filter was then placed in tryptone bile x-glucuronide (TBX) agar medium (Biokar Diagnostics; appendix 1) and incubated overnight at 36 ºC ± 1 ºC. Single colonies of green color were then isolated by streaking in TBX agar and grown overnight at 36 ºC ± 1 ºC. A single colony was then plated in trypticase soy agar (TSA; Biokar Diagnostics, appendix 1) and grown overnight in the same conditions.
- *Enterococcus*: the same initial procedure as *E. coli* was used, with the filter being incubated in Slanetz-Bartley medium (Oxoid, appendix 1). After 48 h of growth at 36 ºC ± 1 ºC, the filters were placed in bile esculin agar medium (Biokar Diagnostics, appendix 1), and grown for 2 h at 44 ºC. Black colonies, presumptively identified as *Enterococcus*, were then isolated by streaking in TSA and grown overnight at 36 ºC ± 1 ºC.
- *S. aureus*: the water sample was filtered through a 0.45 µm pore filter; the filter was then placed in Chapman – mannitol salt agar (Biogerm, appendix 1) and incubated for 48 h at 37 ºC ± 1 ºC. Colonies with a yellow halo were isolated in nutrient agar (Biokar Diagnostics, appendix 1), and subjected to confirmatory tests. These tests included Gram staining, observation of catalase production, testing for aerobic/anaerobic growth using the triple sugar iron test (BD, appendix

1) at 37 ºC for 24 h, and coagulase production, by inoculation into rabbit blood plasma with ethylenediaminetetraacetic acid (EDTA) for 24 h at 37 ºC ± 1 ºC. A Gram positive, catalase positive, facultative anaerobe (verified by the growth from surface to bottom on the previously described test), coagulase positive (verified by the formation of a clot) colony was presumptively identified as *S. aureus*, isolated by streaking in TSA, and incubated overnight at 36 ºC ± 1 ºC.

- *P. aeruginosa*: water samples were filtered through a 0.45 µm pore filter and incubated in CN agar (Biogerm, appendix 1) for 48 h at 36 ºC ± 1 ºC. Green colonies were presumptively identified as *P. aeruginosa*, isolated by streaking in TSA and incubated overnight at 36 ºC ± 1 ºC.

Each of the final isolates was inoculated into a mixture of 90% tryptic soy broth (TSB; BD; appendix 1) and 10% glycerol and stored at -80 ºC ± 10 ºC until used in the antibacterial activity essays.

2.2. Calcium fluoride nanoparticles

2.2.1. Synthesis: CaF_2 NP were produced by co-precipitation of sodium fluoride with calcium chloride using the procedure with minor modifications described by Estrada (Estrada, 2017) (equation 2.1).

$$2\ NaF + CaCl_2 \rightarrow CaF_2 + 2\ NaCl \quad (2.1)$$

Calcium fluoride is highly insoluble in water (National Center for Biotechnology Information, 2020), precipitating rapidly, removing it from the reaction medium and therefore favoring the reaction. Briefly, a 20 g L^{-1} solution of polyvinylpyrrolidone (PVP) 40000MW was prepared using a vortex mixer and a sonication bath. Using the PVP solution as the solvent, two additional solutions were produced: a 0.248 mol dm^{-3} solution of NaF and a 0.166 mol dm^{-3} solution of $CaCl_2 \cdot 2H_2O$. Using two separation funnels, adapted with 1000 µL micropipette tips to decrease the droplet size, 25 mL of the previously prepared NaF and $CaCl_2 \cdot 2H_2O$ solutions were simultaneously added dropwise, while mixing, to 25 mL of PVP solution. The resulting solution was mixed for 2 h, after which 2.30 g of NaCl were added to improve the precipitation of the nanoparticles; the mixture was centrifuged for 10 min at 5000 rpm (VWR Compact Star CS4). The resulting pellet was recovered and washed with a solution of 70% acetone: 30% water (v/v), in order to remove residual salts, using a vortex mixer and sonication bath; the resulting suspension was centrifuged for 3 min at 6000 rpm; this process was repeated five times. The pellet was resuspended in the water acetone mixture, and left to dry in a desiccator. The resulting solid was recovered into an air-tight container and stored at room temperature. Several variations of this process were made, in an attempt to produce nanoparticles (schematical representation in appendix 2):

- 1st batch: the addition of $CaCl_2 \cdot 2H_2O$ and NaF was conducted over the period of 2 h, under mixing at 200 rpm; the 2 h period of mixing that followed was made at 300 rpm.
- 2nd batch: the reagents were added over the period of 10 min, under mixing at 900 rpm; the 2 h period of mixing was made at 1100 rpm.
- 3rd batch: the protocol from the 2nd batch was followed, but the particles were suspended in filtered acetone (0.2 µm syringe filter) and kept on a closed vial instead of drying. The concentration of the suspension was calculated by drying and measuring the mass of 100 µL of suspension.
- 4th batch: particle synthesis was made without PVP coating: both $CaCl_2 \cdot 2H_2O$ and NaF solutions were prepared with water and added to 25 mL of water; the remaining protocol was the same as the 3rd batch.
- 5th batch: the protocol for the 2nd batch was followed, but the batch was subdivided: to the first half of the batch, 1.15 g of NaCl was added whereas the second suffered no other processing. Both suspensions were stored as is, with no washing or removal of the reaction medium.

2.2.2. Characterization: the distribution of particle sizes was determined by dynamic light scattering (DLS; Malvern Zetasizer Nano). For the 1st and 2nd batches, a small amount of nanoparticle powder was suspended in filtered acetone and mixed with the help of a vortex mixer. The resulting suspension was left idle for a short period of time to allow the settling of macroscopic agglomerates of particles, and thus reducing their impact on the evaluation of particle size. Large agglomerates would be detrimental to the measurement, as they were larger than the range of the equipment; in addition, in DLS, larger agglomerates have a disproportional effect on the obtained results (Vogel et al., 2003). Measurements were made in acetone, except when otherwise noted, as this solvent would be used during membrane production. For the 3th and 4th batches, a sample from the suspension was diluted in acetone and measured directly. The measurement of the two final suspensions obtained from the 5th batch was made in water after dilution in this solvent. Five sets of measurements were performed for samples of the 1st, 2nd and 3rd batches; three sets of measurements were used for the 4th and 5th batches. The results were analyzed with Zetasizer Software (Malvern Panalythical).

2.2.3. Antibacterial activity: previous to the production of fluoride nanocomposite membranes, calcium fluoride nanoparticles were tested for antibacterial activity. The effect of pH on nanoparticle activity was evaluated with the 2nd batch of nanoparticles. *E. coli* WDCM 00013 was grown overnight in 10 mL of 1:10 diluted TSB at 37 ºC ± 1 º C in an orbital shaker at 200 rpm; 1 mL of the resulting culture was inoculated in 90 mL of 1:10 diluted TSB, grown for 3 hours in the same conditions and subsequently diluted with medium to approximately 10^5 colony forming units per milliliter (cfu mL^{-1}). Two pH conditions were evaluated: the original pH of the medium (pH 7.3 ± 0.2) and pH 5.5 ± 0.01, adjusted with 5N HCl (pH measured with Hanna instruments HI2212). Nanoparticles were tested at a concentration of 1 mg mL^{-1}. A negative control (same conditions without the addition of fluoride nanoparticles) was also carried out. The nanoparticles were sterilized, prior to usage, by exposure to UV light for a total of 45 min, mixing once during the sterilization period. The assays were performed in 9 mL of 1:10 diluted TSB to which 1 mL of the *E. coli* suspension (10^5 cfu mL^{-1}) was added. The cultures were grown for 116 h, at 26 ºC ± 1 ºC in an orbital shaker at 200 rpm. The growth was evaluated periodically by the plate count method: 150 µL of cell suspension was collected and centrifuged (Eppendorf Minispin Plus) for 1 min at 1000 rpm to pellet the nanoparticles; following centrifugation, dilutions were performed in SDW, 100 µL were plated in TSA and grown overnight at 36 ºC ± 1 ºC. Colonies were counted after this incubation period. Nanoparticle containing essays were performed in duplicate; a single control was used for each pH.

Due to differences in aggregation and size between the dried and suspended nanoparticles, the 3rd batch of nanoparticles was also tested, although only at the original pH of the medium. For this batch, the nanoparticle suspension was washed to remove acetone by centrifugation for 1 min at 5000 rpm, the supernatant was discarded, and the pellet resuspended in SDW; this process was repeated three times. The resulting suspension was UV sterilized as described previously. The remaining procedure was the same used for the 2nd batch of nanoparticles, including nanoparticle concentration.

2.3. Silver nanoparticles

2.3.1. Synthesis: Ag NP were produced via the reduction of silver nitrate with sodium borohydride (equation 2.2)(Sonawane et al., 2017).

$$AgNO_3 + NaBH_4 \rightarrow Ag^0 + \frac{1}{2} H_2 + \frac{1}{2} B_2H_6 + NaNO_3 \qquad (2.2)$$

A 0.01 g mL^{-1} solution of PVP 40000MW was prepared with ultrapure water, to a final volume of 16 mL, which was then used to prepare 8 mL of 0.734 mol dm^{-3} $AgNO_3$ solution and 8 mL of 0.199 mol dm^{-3} $NaBH_4$. Both solutions where subjected to sonication (in a sonication bath) to decrease the amount of dissolved gas. The sodium borohydride solution was added dropwise into the silver nitrate

solution, under constant hand stirring and sonication; this process took less than 2 min. The reaction quickly produced a dark-brown foamy suspension. The suspension was transferred to a brown vial and kept at 4 ºC until further used.

2.3.2. Characterization:

- Absorbance spectrum: a small sample of the Ag NP suspension was diluted in ultrapure water; the absorbance spectrum of the suspension was traced between 190 nm and 900 nm (Shimadzu UV-1700 PharmaSpec). Ag NP have a characteristic peak of absorbance at approximately 400 nm, with suspensions containing agglomerates producing peaks at longer wavelengths (Tejamaya et al., 2012).
- DLS: Particle size distribution was determined by DLS (Zetasizer Nano): a small sample of Ag NP suspension was dissolved in ultrapure and filtered (0.2 µm syringe filter) water. Five sets of measurements were produced per sample. The results were analyzed with Zetasizer Software (Malvern Panalythical).

2.4. Asymmetrical cellulose acetate membranes

2.4.1. Synthesis: asymmetrical cellulose acetate ultrafiltration membranes with different silver contents where produced using the wet-phase inversion process, as described by Figueiredo *et al.* (Figueiredo et al., 2015). The proportions of cellulose acetate, formamide and acetone were the same for all membranes if silver suspension is excluded. All membrane casting solutions contained approximately 30 % of total mass of formamide. Composition of the membrane casting solutions is presented in table 2.2. The silver content in the membranes included not only Ag NP but also any non-reduced silver nitrate contained in the Ag NP suspension. The required mass of nanoparticle suspension was calculated based on the assumption of a complete recovery of silver/silver nitrate during particle synthesis. Thus, a final concentration of silver compounds in the suspension of 39.59 mg mL^{-1} is considered. The density of the suspension, determined by measuring the mass of 1 mL of the suspension, was 0.9747 g mL^{-1}. The different casting solutions were prepared by sequential addition of cellulose acetate, formamide, acetone and Ag NP suspension, followed by a brief mixing to ensure that all cellulose acetate was in suspension and an overnight mixing in an orbital shaker. The casting solutions were prepared in sealable containers to prevent the volatilization of the solvents.

Table 2.2 - Casting solution composition.

Membrane		CA400-30	CA400-30 Ag 0.1	CA400-30 Ag 0.4
% Mass	Cellulose Acetate	17	16.4	15.3
	Acetone	53	51.1	47.7
	Formamide	30	29	27
	Ag NP suspension		3.5	10
	Silver content		0.14	0.4

A casting knife, with a 0.25 mm gate (figure 2.1) and a scratch-free glass panel where both washed with de-ionized water and acetone and cleaned of all debris. The casting knife was then placed on the glass panel, with the gate against the panel and turned toward its closest extremity. The casting solution was placed inside the reservoir of the casting knife until the surface was covered. The casting knife was quickly dragged across the surface of the panel, leaving an even layer of casting solution (figure 2.2). The panel was left still for 30 s and then placed in a cold de-ionized water bath (4 ºC) until the cellulose acetate completely coagulated, forming the membrane. The membrane was separated from the glass panel, the active layer face was marked, and stored in de-ionized water at 4 ºC. The membrane casting was performed at room temperature (23 ºC to 26 ºC) and relative humidity of 42% to 66%.

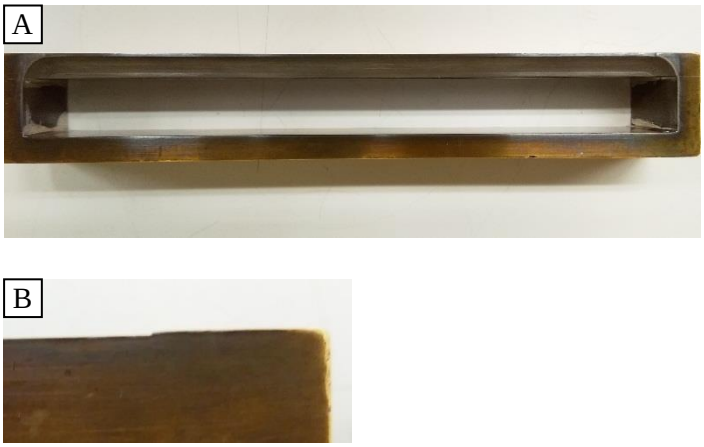

Figure 2.1 – A) Casting knife, viewed from the underside; B) Detail from the side of the casting knife, displaying the 0.25 mm gate.

Figure 2.2 – CA400-30 Ag 0.4 membrane after casting.

2.4.2. Membrane characterization: The three membrane types were evaluated for their hydraulic and separation properties, namely: hydraulic permeability, molecular weight cut-off (MWCO) and salt rejection. All tests were performed on a CELFA P-28 unit (figure 2.3). The CELFA P-28 unit is composed by a 500 mL reservoir, connected to a membrane cell through a pump; it works in crossflow, with the concentrate being recirculated to the reservoir. The permeate is recovered in a separate container. The flow rate/TMP in the membrane cell can be controlled by both the pump speed (represented numerically in its controls) and the position of the valve connecting the membrane cell to the reservoir (regulating valve). The temperature inside the reservoir is regulated by circulating water in a chamber surrounding the reservoir. A circular membrane, with a diameter of 75 mm, is placed inside the membrane cell, with a paper filter of the same size acting as a spacer between the membrane and the porous surface of the bottom of the cell. Inside the cell, the flow proceeds, when in contact with the membrane, through a winding path, resulting in a usable membrane area of 25.52 cm^2 (figure 2.3 C) Before the first use, all membranes must be subjected to compaction. This was performed by filtering de-ionized water at a pressure of 4 bar and a feed mass flow rate of 13.68 g s^{-1} for 2 h.

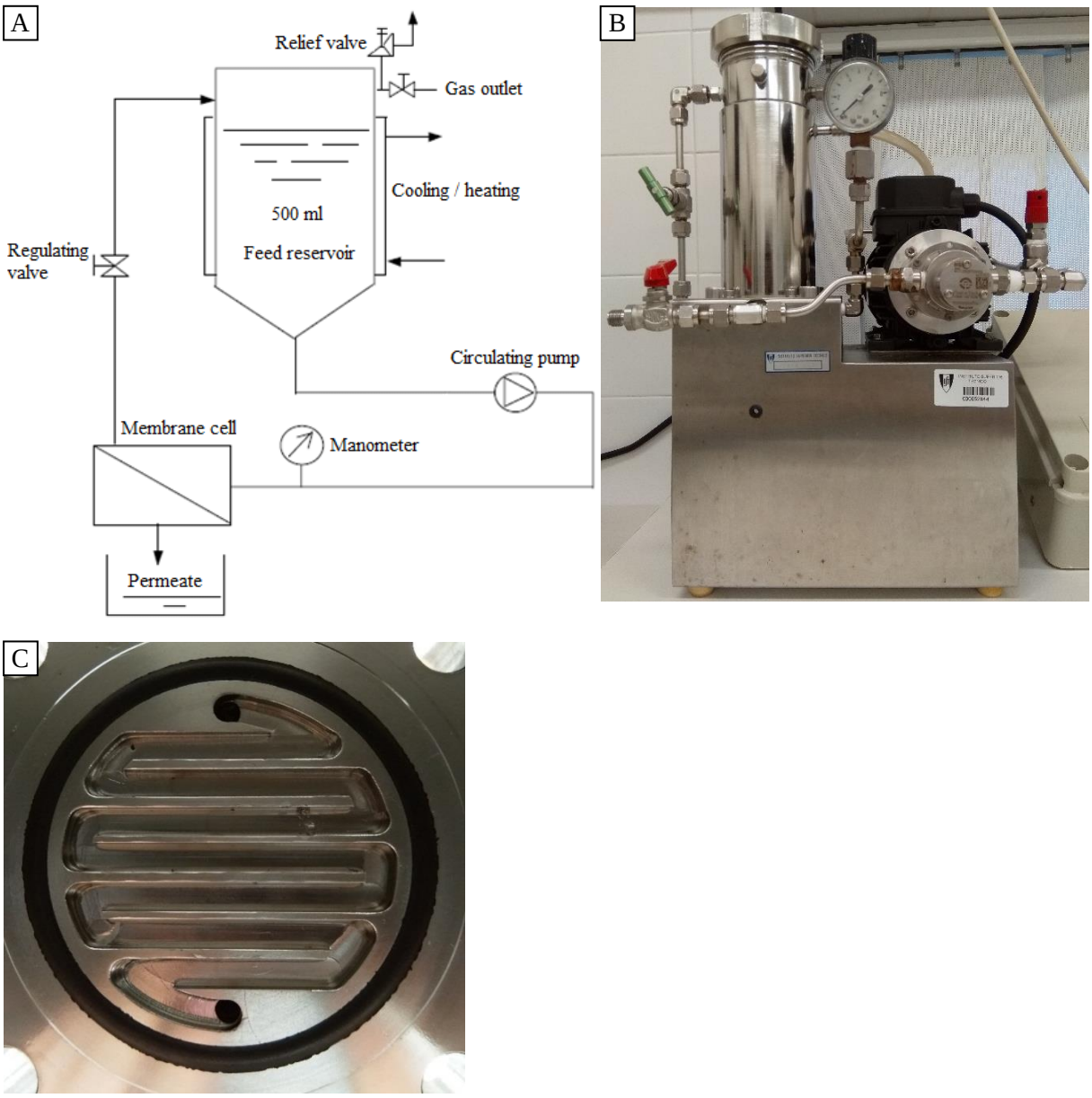

Figure 2.3 – A) Schematic representation of a CELFA P-28 unit; Adapted from de Sousa *et al.* (de Sousa et al. 2014); B) CELFA P-28 unit; C) Upper side of the membrane cell.

CELFA calibration: for the determination of membrane parameters such as the hydraulic permeability, a fixed feed flow rate must be established, independent of the TMP. The first step is therefore to determine, for a given pressure, the changes observed in the feed flow rate with varying pump speed. To that end, using a compacted CA400-30 membrane, the deposit was filled with de-ionized water and the pump was set to a given speed and left for 5 to 10 min to stabilize the feed flow rate; the pressure was then set with the regulating valve. A sample from the concentrate was taken and weighted; the sample collection process was timed. Feed mass flow rate (Q_f; g s^{-1}) was calculated by dividing the mass of the recovered sample by the duration of the sampling (equation 2.3).

$$Q_f = \frac{m}{t} \quad (2.3)$$

This process was repeated in triplicate for several pump speeds at each pressure, until the increase in speed led to an increase in pressure that could not be regulated by opening the valve. A plot with feed mass flow rate versus pump speed was produced for each pressure point (0.5 bar, 1 bar, 1.5 bar, 2 bar, 2.5 bar and 3 bar. Appendix 3).

Hydraulic permeability: hydraulic permeability (L_p; kg h^{-1} m^{-2} bar^{-1}) is defined as the slope of the linear regression obtained by plotting the variation of permeate flux versus the variation of TMP. Permeate flux (J_p; kg h^{-1} m^{-2}) was calculated by dividing the permeate mass flow rate by the area of the membrane (equation 2.4).

$$J_p = \frac{m}{t \times a} \tag{2.4}$$

Hydraulic permeability was determined on a compacted membrane, at a fixed feed mass flow rate of 5 g s^{-1} (achieved by selecting the appropriate pump speed via the CELFA calibration plots) with de-ionized water. Permeation flux was determined for 0.5 bar, 1 bar, 1.5 bar, 2 bar, 2.5 bar and 3 bar. After setting pump speed and TMP, the entire unit was allowed to stabilize for 15 min. While timing the process, the permeate was sampled and then weighted. Three replicas were taken for each pressure.

Molecular Weight Cut-Off: MWCO is defined as the molecular mass of an organic polymer for which a 90.9% rejection coefficient (f; equation 2.5) is obtained for the membrane.

$$f = \frac{c_{deposit} - c_{permeate}}{c_{deposit}} \tag{2.5}$$

To evaluate the MWCO, the permeability of polyethylene glycol (PEG) polymers with an increasing molecular mass was determined for each membrane at 1 bar of TMP and 5 g s^{-1} feed mass flow rate. To that end, solutions of PEG 3000, PEG 6000, PEG 10000, PEG 20000 and PEG 35000 with a final concentration of 0.6 g L^{-1} were prepared in ultrapure water. MWCO for CA400-30 was determined using the PEG 3000 through PEG 20000 solutions; MWCO for CA400-30 Ag 0.1 and CA400-30 Ag 0.4 was determined using all PEG solutions. The deposit of the CELFA unit was filled with a solution of PEG; the unit was then operated for 40 min at 1 bar and 5 g s^{-1} feed mass flow rate; afterwards the permeate collected during this time was added back to the deposit, thus ensuring that the concentration of PEG was homogeneous in the unit. The deposit was sampled followed by the sampling of the permeate; this sampling process was repeated three times for each PEG solution. The rejection coefficient for each PEG solution was determined as the ratio of total organic carbon (TOC) present in the permeate in relation to the TOC of the solution in the deposit (calibration plots in appendix 4). TOC was evaluated using a Shimadzu TOC-VCSH. TOC is evaluated through the quantification of CO_2 generated by the oxidation of the sample. The $\log_{10}(f/(1-f))$ for each PEG solution was plotted versus the molecular mass of each PEG; the MWCO was determined by the intersection of the linear regression obtained with the plot with y=1 (approximation of $\log_{10}(0.909/(1-0.909))$.

Salt permeability: salt rejection coefficients were determined for sodium chloride and sodium sulfite, by evaluating the salt concentration in the solution contained in the deposit and the permeate (equation 2.5). Salt concentrations were determined by measuring the conductivity of the solutions, using a Crison GLP 32 conductivity meter (calibration plots in appendix 5). Salt rejection was evaluated at 1 bar of TMP, with a feed mass flow rate of 5 g s^{-1}. A 0.6 g L^{-1} solution of each salt was prepared with de-ionized water and placed in the deposit of the CELFA unit containing a compacted membrane. The unit was operated for 45 min to stabilize the permeate flux and the concentration of salt inside the unit, retuning the permeate to the deposit at the end of this period. The deposit and three samples of permeate were obtained. Conductivity measurements were performed in triplicate. Each sample was added to the deposit before the next sample was obtained.

2.4.3. Membrane antibacterial activity: The effects of the membranes, CA400-30, CA400-30 Ag 0.1 and CA400-30 Ag 0.4, on the growth kinetics of bacteria were first evaluated for the laboratory strains of *E. coli*, *E. faecalis*, *S. aureus* and *P. aeruginosa*. Afterwards, using a methodology adapted for a larger throughput of results, the environmental isolates were screened for resistance to the silver-

containing membranes, CA400-30 Ag 0.1 and CA400-30 Ag 0.4; the laboratory strains were also tested to ensure consistency in the results between the two methodologies.

Growth kinetics: before use, each membrane was cut into a circle with a diameter of 47 mm, and sterilized by UV exposure, 30 min per side, in SDW. Each strain was grown overnight in TSB at 37 ºC ± 1 ºC in an orbital shaker at 150 rpm, subsequently diluted 1:10 in fresh TSB and left to grow for 3.5 h ± 0.5 h under the same conditions. The resulting culture was diluted in TSB to an optical density (OD) of approximately 0.1 at 600 nm (Techcomp UV 1102 Spectrophotometer) and then further diluted 1:10 in TSB. One-milliliter of the resulting dilution was inoculated in 9 mL of autoclaved tap water in sterile cups containing the membrane (or without a membrane as a control) This resulted in an initial bacterial concentration of 10^6 cfu ml^{-1}, in a 1:10 diluted TSB medium. Tap water was used since these membranes are expected to be applied in this particular matrix; the greater concentration of salts and organic compounds in this water when compared to de-ionized water should imposed some of the potential limitations described previously in section 1.3.2. Each bacterial strain was incubated in an orbital shaker, at 37 ºC ± 1 ºC and 150 rpm. Growth was evaluated by periodic sampling at 30 min, 90 min, 150 min of growth, and following overnight incubation (approximately 19 h). Evaluation of the antibacterial activity was performed by plate counting. Culture samples were serially diluted with SDW; 100 µL of appropriate dilutions were plated in TSA and incubated overnight at 37 ºC ± 1 ºC. This procedure was repeated for *E. coli* WDCM 00013, replacing TSB with maximum recovery diluent (MRD; BD, appendix 1), to simulate a nutritionally poor environment. The assays were performed in triplicate for each membrane/control and bacterial strain tested.

Resistance screening: 1 cm^2 square membrane pieces were sterilized by UV for 30 min each side in SDW. Each isolate/laboratory strain culture suspension was prepared in TSB diluted in sterile tap water, to a final volume of 10 mL, using the previously described protocol. To maintain the membrane area to suspension volume ratio, 0.55 mL of the suspension were added to the membrane (or none as a control), in a 2 mL centrifuge tube, and incubated for 19 hours at 37 ºC ± 1 ºC with mixing at 150 rpm. Growth was evaluated by determining the OD of the culture, using a 96-well microplate and microplate reader at 620 nm (Labsystems iEMS Reader MF). Experiments were conducted in triplicate for all membranes/controls for each isolate/strain.

3. Results and Discussion

3.1. Calcium fluoride nanoparticles

Particle size distributions for each batch of CaF_2 particles are presented in figure 3.1.

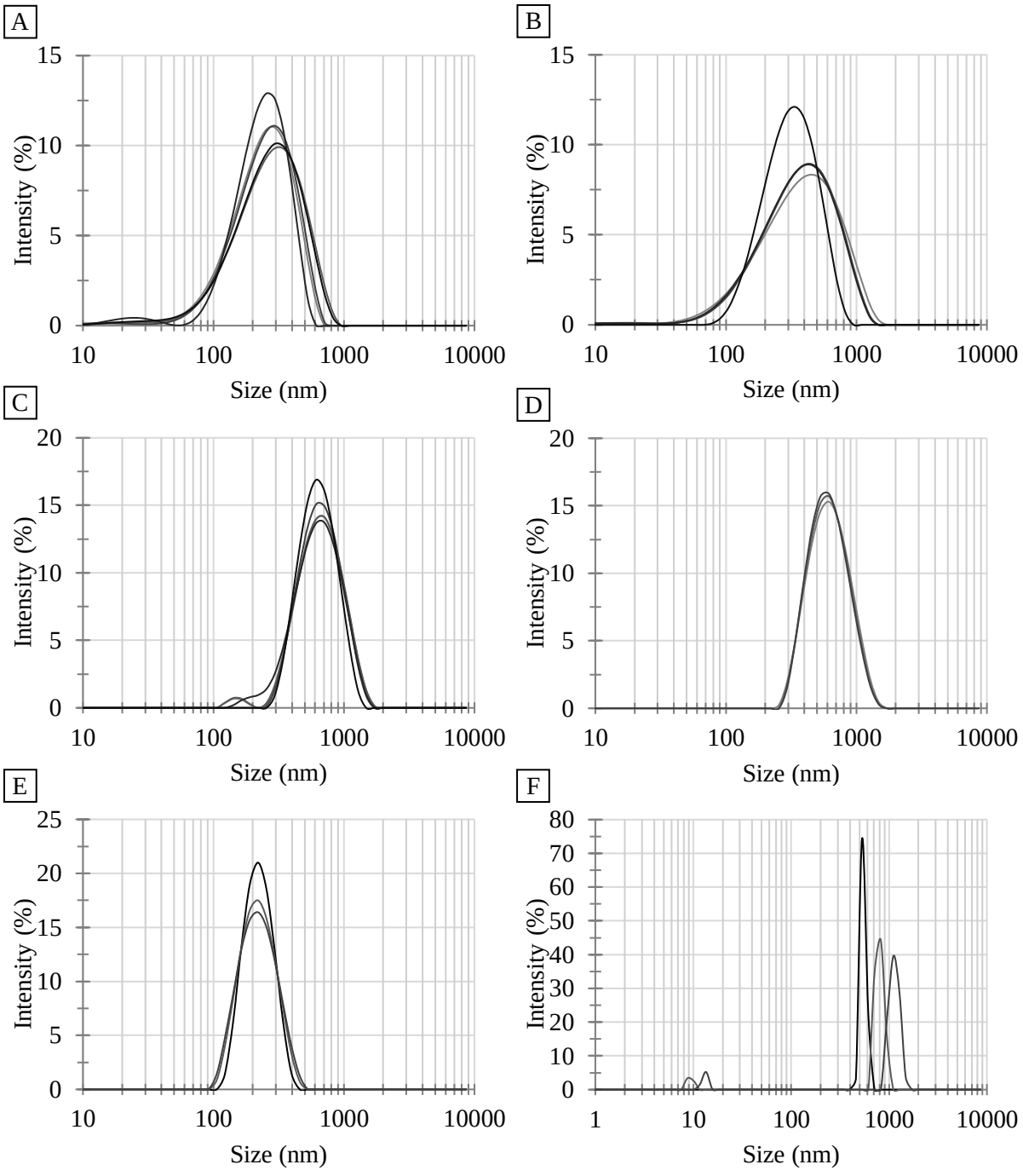

Figure 3.1 – CaF_2 particle size distributions, obtained with DLS. Each line represents one set of measurements. A) 1st batch; B) 2nd batch; C) 3rd batch; D) 4th batch; E) 5th batch, without NaCl; F) 5th batch, with NaCl.

DLS measurements report the size of spheres with the same dynamic properties in a given solvent as the particle being measured, resulting in similar or slightly larger size estimates (Bootz et al., 2004). All dried particles - 1st and 2nd batches - presented macroscopic aggregates of particles that did not disperse with mixing and sonication when resuspended in acetone or water; these aggregates are not included in the size distribution. Although the 1st batch had, on average, smaller suspended particles than the 2nd batch – peak height of 300 nm for the 1st batch and 450 nm for the second batch on size

distribution charts – the 1st batch contained a larger number of visible aggregates. As the two batches differed in rate of reagent addition and on solution mixing speeds, these factors may have an impact on the production of nanoparticles. In comparison, the 3rd batch of particles had larger particles in suspension – 600 nm peak height – accounting for all of the particles produced, as no macroscopic particles were visible. Particles produced without PVP (4th batch) and left in suspension had a similar size distribution to the 3rd batch of particles. The 5th batch of particles, without the addition of NaCl following synthesis, contained overall the smallest particles, with a size distribution peak height at 220 nm. The results obtained for the 5th batch with NaCl are not representative of the real size of suspended particles – the three disparate sets of measurement are an indication that large agglomerates of particles were present in the suspension. Several conclusions can be drawn from these data. None of the CaF_2 particles produced fit the definition of nanoparticles, defined as particles with, at least, two dimension with a size between 1 nm and 100 nm (Vert et al., 2012) (particles slightly larger than 100 nm are sometimes reported in literature as nanoparticles). Instead, the particles synthetized are classified as calcium fluoride microparticles (CaF_2 MP). None of the variations of the particle synthesis protocol successfully replicated the results obtained by Estrada (Estrada, 2017), where particles with an average size of 110 nm were obtained. The addition of NaCl led to the aggregation of the particles, which was (at least partially) reverted during particle washing. The suspension was subjected to centrifugation after NaCl addition. Even if the aggregated particles were easier to remove from suspension, a change in the centrifugation protocol would achieve the same result. NaCl addition, therefore, appears to be unnecessary and potentially deleterious in the production of CaF_2 NP by the method described by Estrada (Estrada, 2017). The smaller size of the unwashed particles (5th batch) compared to the washed particles indicates that the particles irreversibly aggregated during washing. PVP is normally added to certain nanoparticles, like Ag NP, as it prevents nanoparticle aggregation (Koczkur et al., 2015). The addition of PVP to the reaction medium did not decrease aggregation, as demonstrated by the similar size of washed particles produced with (3rd batch) and without (4th batch) PVP in comparison to the unwashed, unaggregated particles of the 5th batch.

The growth of *E. coli* WDCM 00013 subjected to CaF_2 MP treatment using the 2nd and 3rd batches of particles is represented in figure 3.2. The 2nd batch was tested as it contained a smaller number of macroscopic agglomerates than the 1st batch; the 3rd batch was tested as it corresponded to the same synthesis protocol as the 2nd batch, altough without drying.

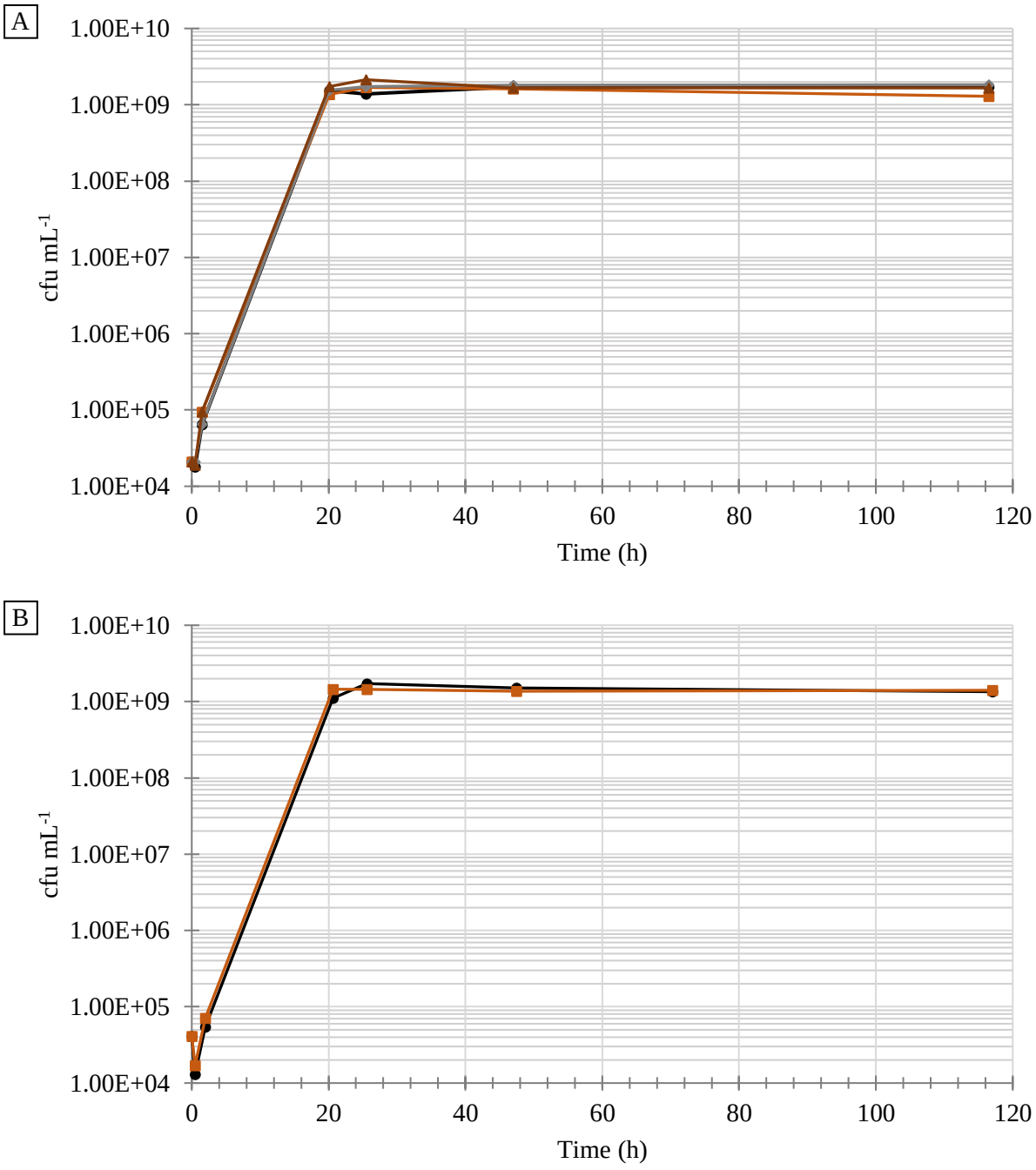

Figure 3.2 – Bacterial growth over time on CaF_2 MP treated *E. coli*. Control values obtained from a single assay. CaF_2 MP assay values represent the average of two replicas. A) Effect of pH on CaF_2 MP activity, using the 2nd batch of particles: ● – Control pH 7.3; ■ – CaF_2 MP pH 7.3; ♦ - Control pH 5.5; ▲ – CaF_2 MP pH 5.5. B) Effect of the 3rd batch of particles: ● – Control; ■ – CaF_2 MP.

Neither batch of particles had any effect on the growth of *E. coli*. Particles were used at a concentration of 1 mg mL^{-1}; for the 2nd batch of CaF_2 MP, this includes both suspended microparticles and macroscopic agglomerates. The concentration of particles used was larger than the minimum inhibitory concentration of 0.2 mg mL^{-1} CaF_2 NP for *E. coli*, reported by Bala *et al.* (Bala et al., 2017). The lack of antibacterial activity might be attributed to the size of the particles. The activity of CaF_2 NP is dependent on the release of fluoride. Larger particles have smaller ratios of particle volume/surface area, which has been linked to reduced F^- release (H. H. K. Xu et al., 2008). Commercial CaF_2 MP tested by Bala *et al.* also lacked antibacterial activity (Bala et al., 2017). The pH of the medium did not have a

noticeable impact on the antibacterial activity of CaF_2 MP. Nonetheless, the influence of pH in the antibacterial activity of CaF_2 NP still has to be evaluated.

The failure to obtain nanoparticles, coupled with the lack of activity of CaF_2 MP in preliminary testing against *E. coli*, ruled out the application of these particles in cellulose acetate ultrafiltration membranes. In view of these results, the antibacterial activity and correspondent potential anti-biofouling effect of the nanocomposite membranes described by Estrada (Estrada, 2017) could not be evaluated.

3.2. Silver nanoparticles

The Ag NP suspension was dark brown and opaque. The absorbance spectrum of the suspension, traced between 190 nm and 900 nm, displayed a single peak at 396 nm, which is indicative of non-agglomerated Ag NP (Tejamaya et al., 2012). The size distribution of the particles, obtained with DLS, is presented in figure 3.3.

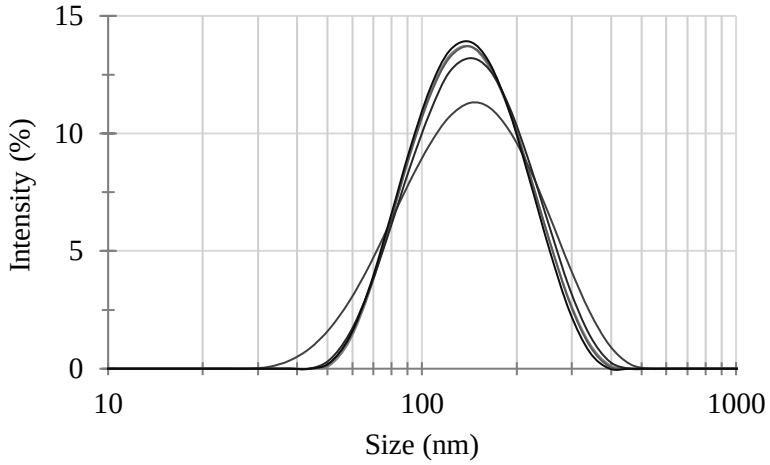

Figure 3.3 – Silver particle size distribution, obtained with DLS. Each line represents one set of measurements.

Part of the size distribution falls outside the typical definition of nanoparticle. Ag NP size distribution featured a single peak at 142 nm. This size distribution is only valid for the nanoparticle suspension and may not be representative of the final particles present in the membrane. Ag NP synthesis was made with an excess of $AgNO_3$. Assuming a complete reaction, 72.9 % of the initial silver nitrate remains in the Ag NP suspension after particle synthesis. As Ag NP were not submitted to washing, a large amount of $AgNO_3$ was present in the casting solution. Formamide is known to reduce $AgNO_3$ into metallic silver, a reaction also used to produce Ag NP (Sarkar et al., 2005). Consequently, production of nanoparticles may also have occurred in the casting solution, and these nanoparticles would not be included in the size distribution obtained with DLS. If nanoparticle formation occurred in the casting solution, the resulting particles were probably not aggregated – Ag NP aggregation changes the color of the suspension from yellow/brown to grey, followed by the formation of a deposit of aggregated particles (Solomon et al., 2007). This was not visible in the casting solutions. Figueiredo *et al.* used scanning electron microscopy to measure Ag NP present on the active layer of CA400-30 Ag 0.1 and CA400-30 Ag 0.4 membranes and reported smaller particles (the majority were below 100 nm) than the DLS analysis in this dissertation (Figueiredo et al., 2015). However, this only accounts for the nanoparticles present on the surface, excluding the particles dispersed on the membrane matrix, and thus cannot be taken as the size distribution of the nanoparticles present in the membrane. Overall, the size distribution of Ag NP present in the final membrane is unknown, but in the membranes produced here it should contain both nanoparticles and particles larger than 100 nm.

3.3. Asymmetrical cellulose acetate membranes

The addition of Ag NP to the casting solution resulted in a change of color of the membranes from transparent to yellow/brown (figure 3.4).

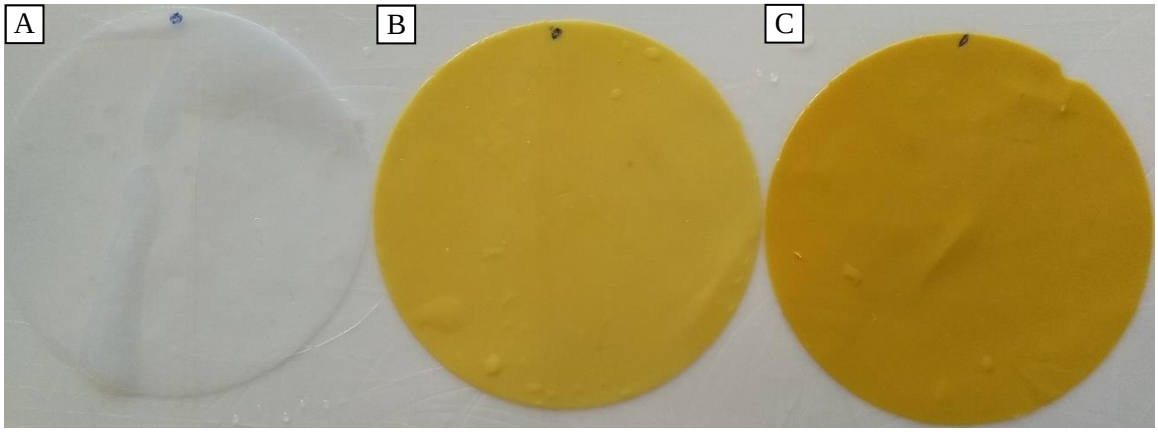

Figure 3.4 – Asymmetrical cellulose acetate ultrafiltration membranes. A) CA400-30; B) CA400-30 Ag 0.1; C) CA400-30 Ag 0.4.

3.3.1. Membrane characterization

Figure 3.5 represents the hydraulic permeability for CA400-30, CA400-30 Ag 0.1 and CA400-30 Ag 0.4.

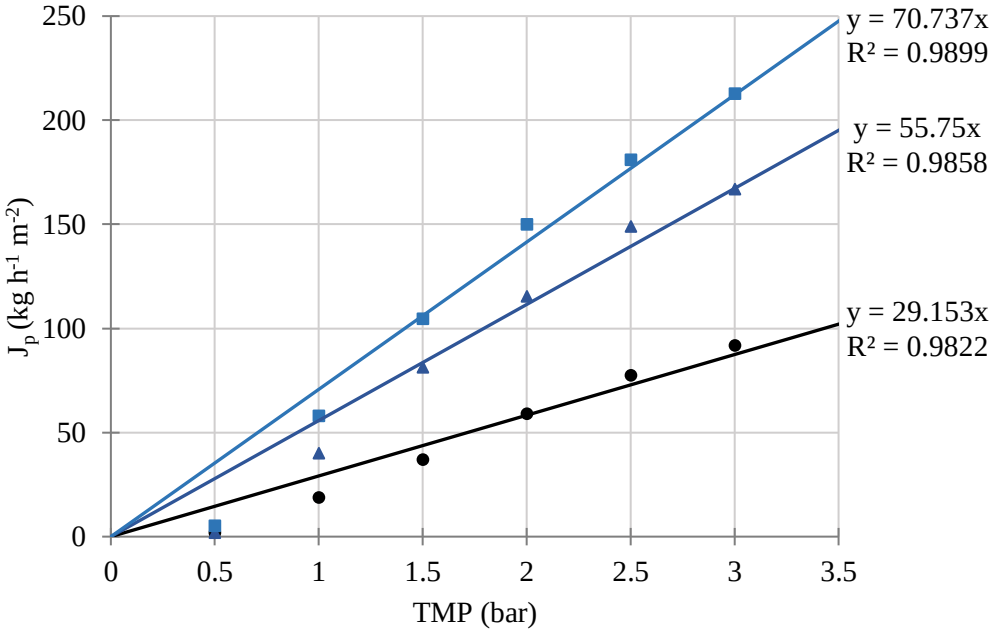

Figure 3.5 – Hydraulic permeability plots: ● – CA400-30, L_p = 29.153 kg h^{-1} m^{-2} bar^{-1}; ▲ – CA400-30 Ag 0.1, L_p = 55.75 kg h^{-1} m^{-2} bar^{-1}; ■ – CA400-30 Ag 0.4, L_p = 70.737 kg h^{-1} m^{-2} bar^{-1}.

Hydraulic permeability increased with the increase in silver content; the same effect was reported by Figueiredo *et al.* (Figueiredo et al., 2015). A higher hydraulic permeability is desirable, as it translates into a larger permeate flux for the same TMP.

Unlike MF membranes, which are typically classified by pore size (either average or largest pore size), UF membranes separation capabilities are measured with MWCO, or the lowest molecular mass of a reference organic polymer with a rejection coefficient of 90.9% (Allgeier et al., 2005). Despite this metric, UF membranes retain molecules/particles based on size. MWCO determination plots are presented in figure 3.6; MWCO are presented in table 3.1 (PEG rejection coefficients in appendix 6).

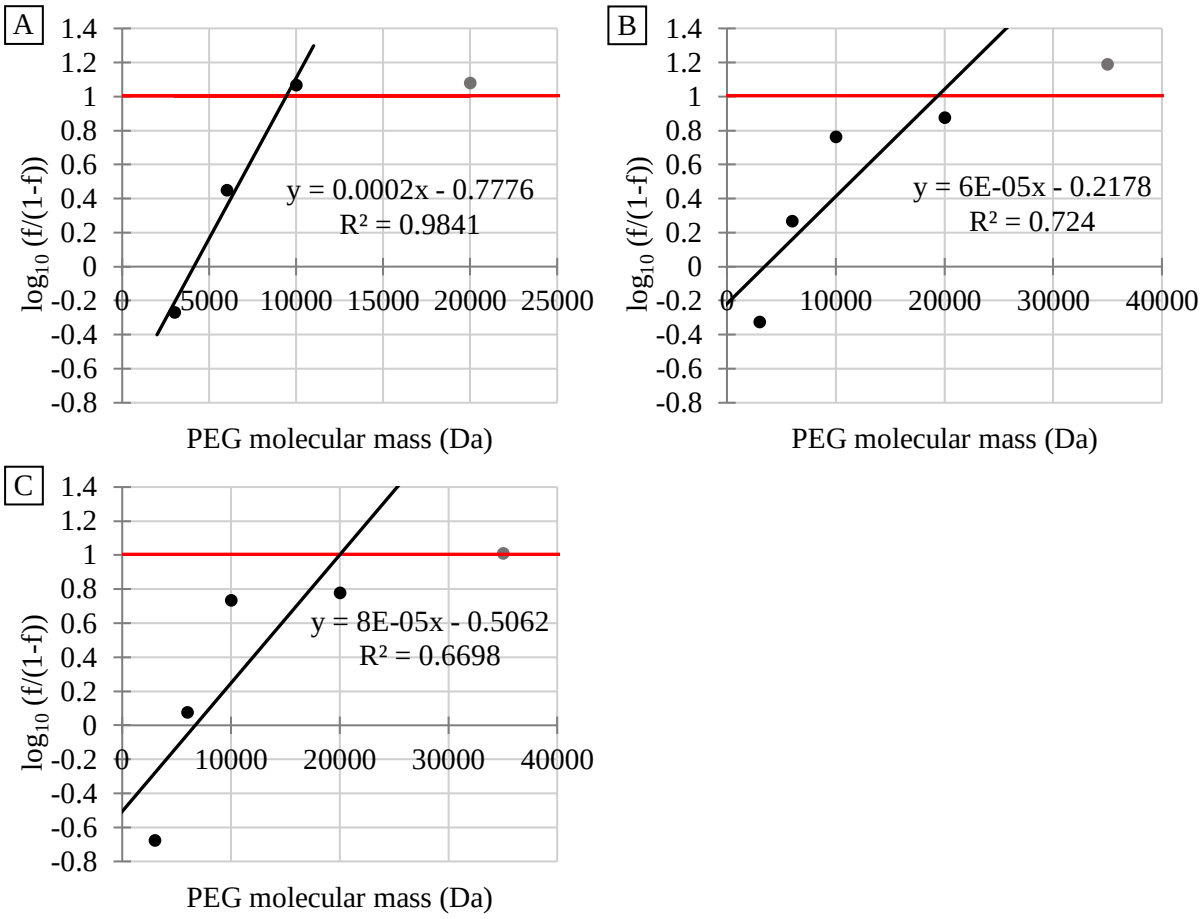

Figure 3.6 – MWCO determination plots. ● – point used in the linear regression; ● – point not used in the linear regression; red line marks a rejection coefficient of 90.9%. A) CA400-30; B) CA400-30 Ag 0.1; C) CA400-30 Ag 0.4.

Table 3.1 – Membrane MWCO.

Membrane	CA400-30	CA400-30 Ag 0.1	CA400-30 Ag 0.4
MWCO (kDa)	8.90	19.4	20.1

UF membranes have a MWCO between 1 kDa and 500 kDa (Crittenden et al., 2012). Therefore, the membranes described here fall into the category of UF. A large increase in MWCO was observed with increasing concentration of Ag NP in the membrane matrix with the difference being considerably smaller for the two silver contents. Similar results were described by Figueiredo *et al.* (Figueiredo et al., 2015). The salt rejection coefficients (appendix 5) for all membranes were small, and consistent with other UF membranes (Figueiredo et al., 2015).

The use of Ag NP nanocomposite membranes presents a trade-off between increased hydraulic permeability and decreased selectivity. The difference in silver content between CA400-30 Ag 0.1 and CA400-30 Ag 0.4, resulted in an increase of 21% in the hydraulic permeability with only an increase of 3.5% in MWCO. Therefore, increasing the content of silver in the membranes would still be justified if similar antibacterial activity were found for both membranes.

3.3.2. Antibacterial activity

The effect of the silver nanocomposite ultrafiltration membranes on the growth kinetics of the laboratory strains of *E. coli*, *E. faecalis*, *P. aeruginosa* and *S. aureus* is presented on figures 3.7, 3.8, 3.9 and 3.10, respectively.

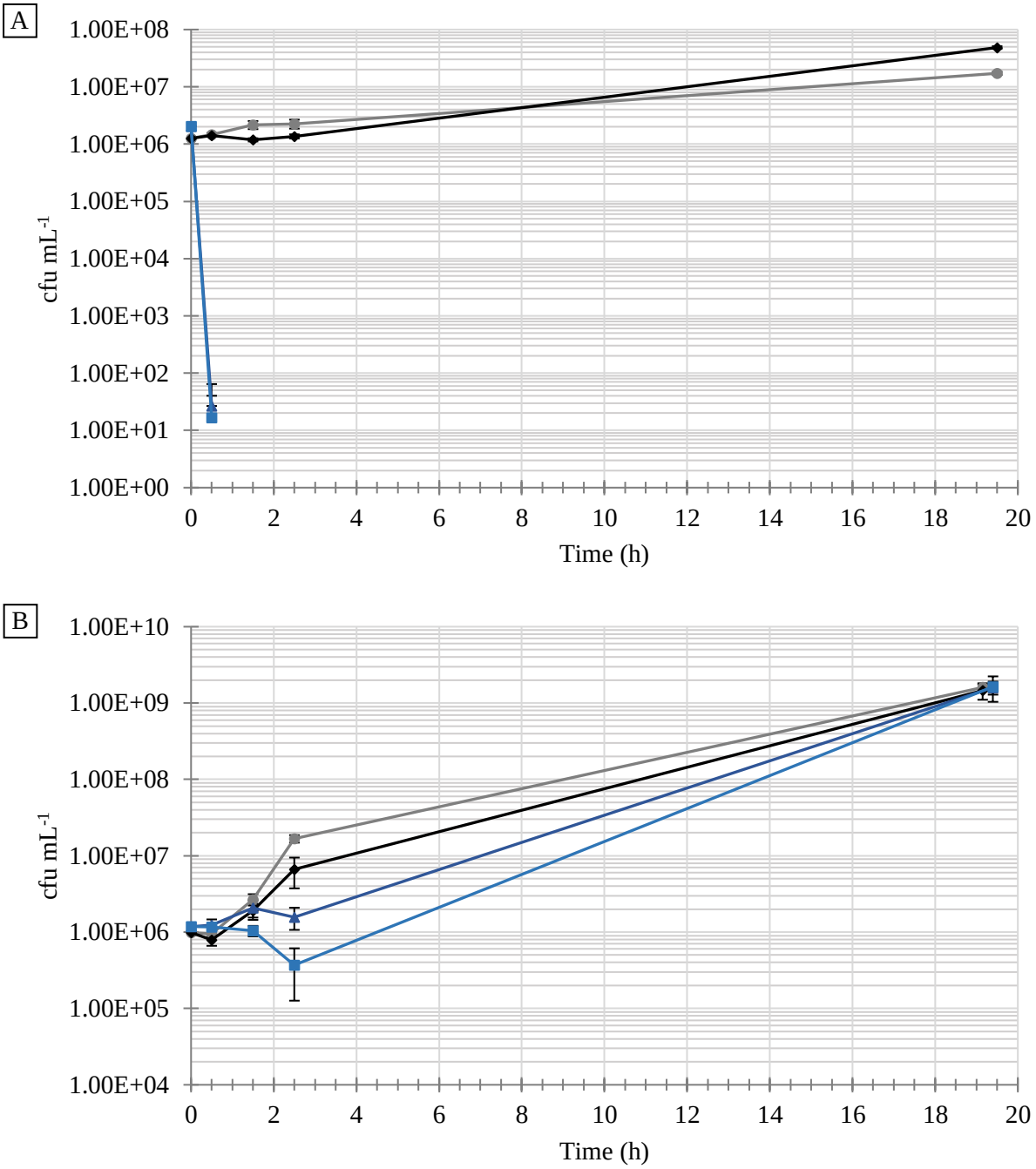

Figure 3.7 – Growth plots for *E. coli* WDCM 00013 treated with Ag NP nanocomposite membranes. ● – Control; ♦ – CA400-30; ▲ – CA400-30 Ag 0.1; ■ – CA400-30 Ag 0.4. Each point represents the average of three replicas. Error bars display standard deviation. A) 1:10 diluted MRD; B) 1:10 diluted TSB.

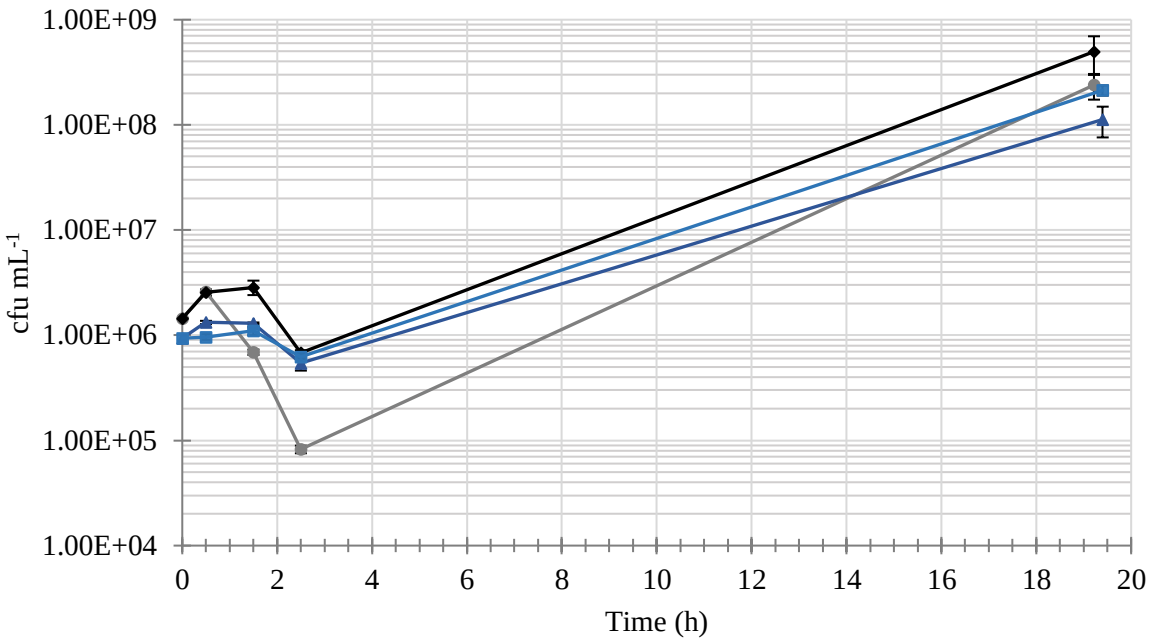

Figure 3.8 – Growth plots for *E. faecalis* WDCM 00009 treated with Ag NP nanocomposite membranes. ● – Control; ♦ – CA400-30; ▲ – CA400-30 Ag 0.1; ■ – CA400-30 Ag 0.4. Each point represents the average of three replicas. Error bars display standard deviation.

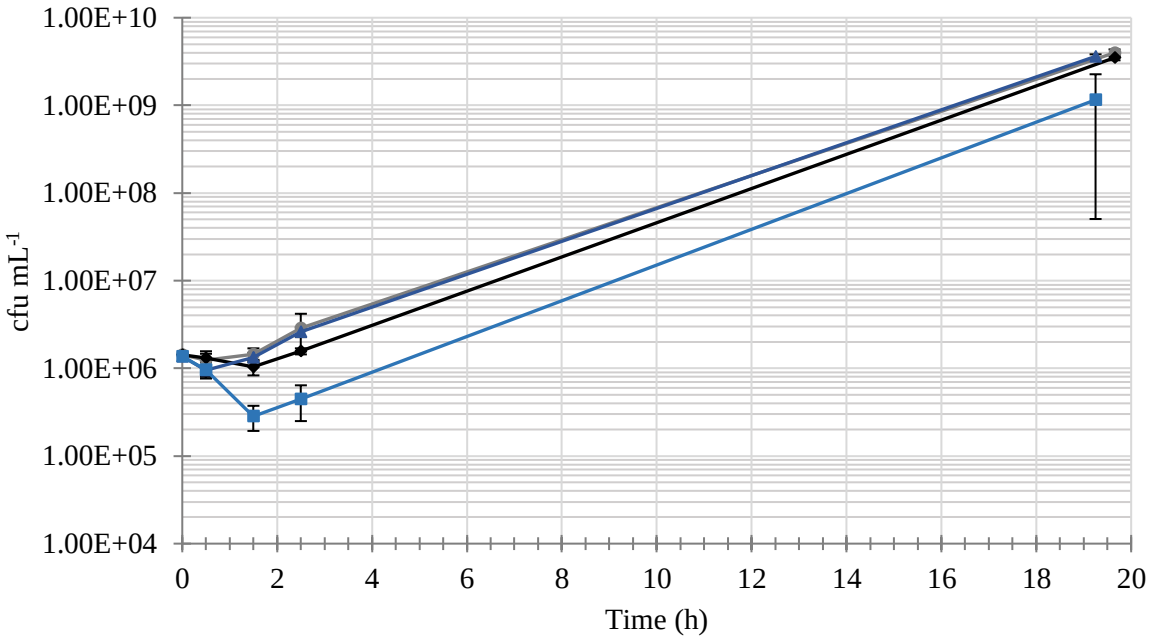

Figure 3.9 – Growth plots for *P. aeruginosa* WDCM 000024 treated with Ag NP nanocomposite membranes. ● – Control; ♦ – CA400-30; ▲ – CA400-30 Ag 0.1; ■ – CA400-30 Ag 0.4. Each point represents the average of three replicas. Error bars display standard deviation.

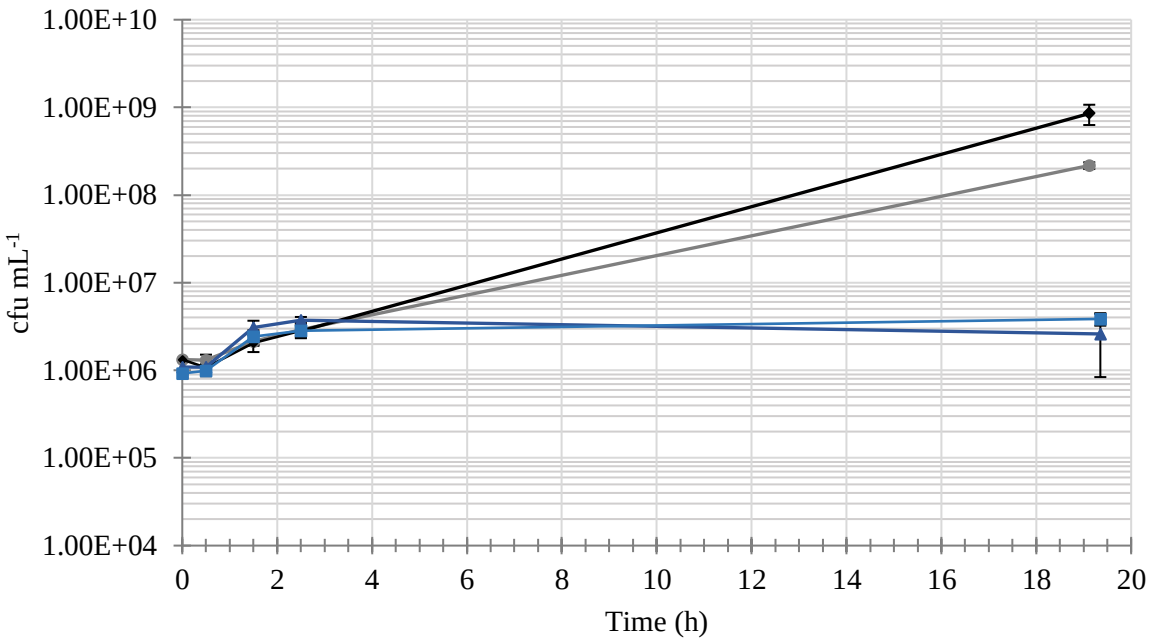

Figure 3.10 – Growth plots for *S. aureus* WDCM 00034 treated with Ag NP nanocomposite membranes. ● – Control; ♦ – CA400-30; ▲ – CA400-30 Ag 0.1; ■ – CA400-30 Ag 0.4. Each point represents the average of three replicas. Error bars display standard deviation.

The activity of Ag NP nanocomposite membranes was dependent on the medium and on the bacteria under treatment. In 1:10 diluted MRD, a complete inactivation of suspended *E. coli* was achieved with CA400-30 Ag 0.1 and CA400-30 Ag 0.4; overall, *E. coli* in 1:10 MRD had decreased growth compared to 1:10 diluted TSB. In 1:10 diluted TSB, with CA400-30 Ag 0.1 membranes, *E. coli* had a reduced growth compared to control at 2.5 h; CA400-30 Ag 0.4 membranes led to a decrease in culturable bacteria in the same period of time. The effects detected in the first hours for each silver containing membranes where not maintained for the remainder of the assay, with similar colony counts for all membranes. The source of the difference in the inactivation of *E. coli* between media is unclear. TSB has a larger concentration of protein than MRD. The antibacterial activity of Ag^+ has been shown to be affected by the composition of the growth medium; tryptone (used as a protein source in TSB), in particular, was shown to decrease the activity of Ag^+ (De Leersnyder et al., 2018). It is also possible that the increased activity of silver in 1:10 dilute MRD was due to the decreased growth rate of *E. coli* in that medium. Ag NP containing membranes had no effect on the growth of *E. faecalis*, with similar final bacterial counts in all assays. In *P. aeruginosa*, CA400-30 Ag 0.4 membranes caused an initial decrease in culturable bacteria, not present in the control. At the end of the assay, however, *P. aeruginosa* had grown to identical final colony counts independently of treatment. The presence of an initial decrease in culturable bacteria for CA400-30 Ag 0.4 in *E. coli* and *P. aeruginosa* grown in 1:10 diluted TSB demonstrates that Ag NP contained in the membranes had some effect on the bacteria, although insufficient to lead to an actual inhibition of growth. *S. aureus* WDCM 00034 was the only strain to show consistent inhibition of growth due to Ag NP, as both silver-containing membranes had a bacteriostatic effect on the cultures. No substantial change in growth can be attributed to CA400-30, indicating that any effect caused by CA400-30 Ag 0.1 and CA400-30 Ag 0.4 can be attributed to silver.

Resistance to silver can vary between strains of the same species (Gupta et al., 1998). Therefore, multiple isolates of each species/genus were tested for resistance to the Ag NP nanocomposite membranes. Resistance screening in environmental isolates is presented in figure 3.11.

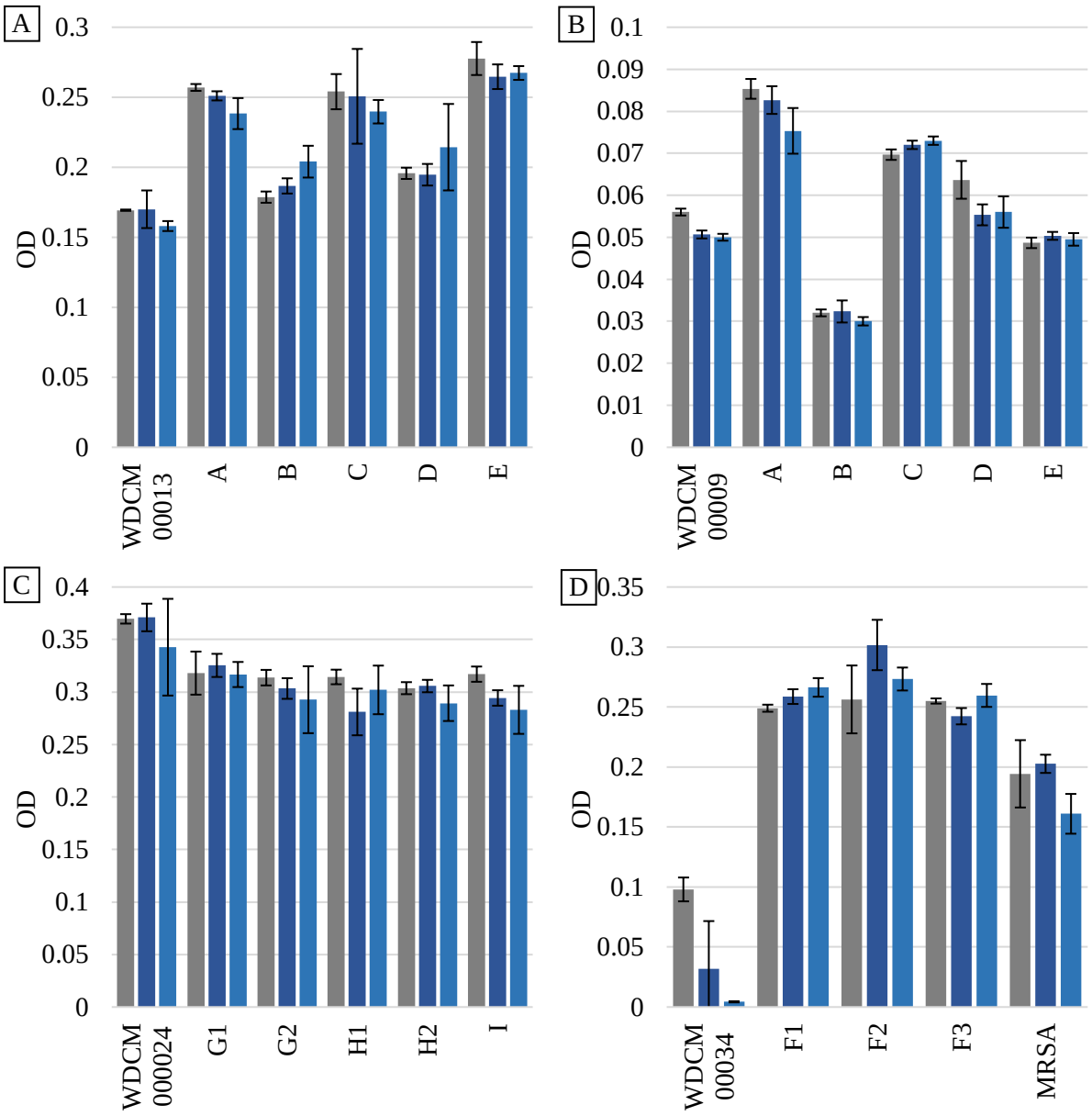

Figure 3.11 – Final optical density of resistance screening tests. ■ – Control; ■ – CA400-30 Ag 0.1; ■ – CA400-30 Ag 0.4. Average values obtained from three replicas. Error bars display standard deviation. A) *E. coli*; B) *Enterococcus*; C) *P. aeruginosa*; D) *S. aureus*.

The bacterial concentration of the suspensions before incubation was under the detection range of the spectrophotometer/microplate reader (bacterial suspension OD was the same as the medium used as blank). Therefore, only the final OD is presented; this limitation also means that this methodology is insufficient to evaluate whether the treatment led to a bactericidal or a bacteriostatic effect. Of all isolates/strains tested, only *S. aureus* WDCM 00034 showed sensitivity to the silver containing membranes. This result confirms that the methodology would lead to the detection of sensitive isolates, if any had been obtained. Silver resistance/sensitivity varied between strains/isolates of *S. aureus*, highlighting the need for testing of multiple strains of the same species.

The antibacterial action of the membranes studied should be mainly due to a diffusible agent, rather than contact with the membrane itself. A complete inactivation of the bacteria, as achieved for *E. coli* WDCM 00013 in 1:10 diluted MRD, would be unlikely otherwise, as it would require a direct contact between every bacterium in the suspension and the nanoparticles fixed on the membrane, at all times. This, however, does not imply that the antibacterial action was just due to Ag^+ leaching resulting

from nanoparticle oxidation. If Ag NP released from the membrane matrix and stayed in suspension, direct contact of Ag NP with the bacteria could still be the mechanism of action. The membranes and the assay medium for the growth kinetics assays of *P. aeruginosa* WDCM 000024 + CA400-30 Ag 0.4 and *S. aureus* WDCM 00034 + CA400-30 Ag 0.1 were kept for 13 days at room temperature (22 ºC), during which the membranes became discolored (figure 3.12), hinting at the loss of silver nanoparticles. This was particularly noticeable with CA400-30 Ag 0.1 (figure 3.12 A), with the membrane becoming closer in color to CA400-30 (as seen in figure 3.4 A) than to its original state (figure 3.4 B). It should be noted that, previously, the same membranes were stored at 4 ºC for eight months without suffering discoloration. The amount of silver leached from a single replica of each membrane was measured by atomic absorption spectroscopy and found to be 0.675 mg L^{-1} for CA400-30 Ag 0.1 and 3.17 mg L^{-1} for CA400-30 Ag 0.4, proportional to the membrane silver content of the membrane. Due to the specifics of the technique, each sample was filtered with a 0.45 µm syringe filter before the silver content was evaluated, so silver bonded to bacteria and large detritus was not accounted in the measurement.

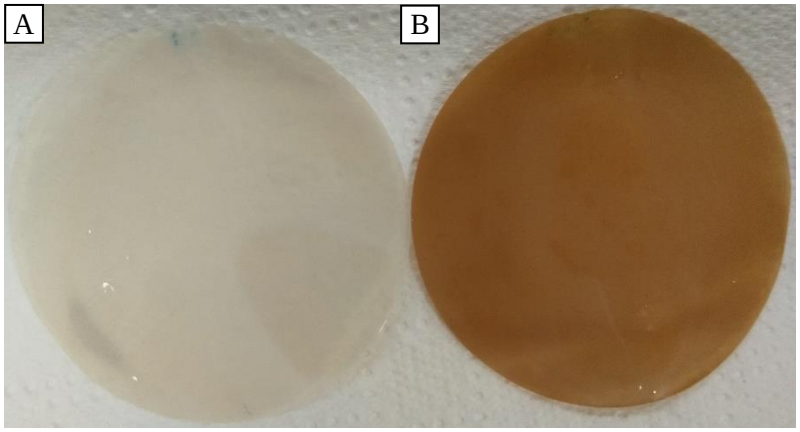

Figure 3.12 – Discolored membranes after 13 day incubation in 1:10 diluted TSB bacterial cultures. A) CA400-30 Ag0.1 incubated with *S. aureus*; B) CA400-30 Ag 0.4 incubated with *P. aeruginosa*.

Silver leaching from the membranes, in the time frame of the assays, was insufficient to achieve the lethal concentration of silver for most bacteria under study. Instead of a neutral effect against biofouling, sub-lethal levels of Ag NP could lead to an increase biofilm production (Yang & Alvarez, 2015) Furthermore, bacteria in biofilms are commonly found to be more resistant to antibacterial compounds, including Ag NP (Sheng & Liu, 2011).

The results obtained for CA400-30 Ag 0.1 and CA400-30 Ag 0.4 are dissimilar from other nanocomposite membranes containing Ag NP produced with the same procedure used here. Beisl *et al.* obtained a 99.95% reduction in *E. coli* after 210 min of treatment with a nanocomposite NF membrane with 0.14% silver in the casting solution (Beisl et al., 2019). Cellulose acetate ultrafiltration membranes with 34% formamide in the casting solution lowered the colony counts of *E. coli* cultures to 1/10 the initial count for CA400-34 Ag 0.1 and less than 1/1000 for CA400-34 Ag 0.4 after 18 h of treatment (Figueiredo, 2016). Both works used 1:10 diluted nutrient broth as the growth medium. If the difference between these results and those obtained for *E. coli* in 1:10 diluted TSB was caused by medium composition, a substantial effect of feed composition in antibiofouling activity is expected in practical applications of these membranes.

4. Conclusion

The failure to obtain CaF_2 NP highlights the need for detailed methodologies in the production of nanoparticles. The reagent addition rates and mixing speed were not reported in the study by Estrada (Estrada, 2017), which may have had an impact on the synthesis of particles; additionally, some steps of the particle synthesis are likely unnecessary, namely the addition of NaCl. Since nanoparticles were not obtained in any stage of the particle synthesis, the action of PVP in preventing CaF_2 NP agglomeration could not be evaluated; nonetheless, PVP revealed to be ineffective in preventing the agglomeration of CaF_2 MP. The lack of antibacterial activity from CaF_2 MP is likely due to the large size of the particles decreasing the amount of fluoride release. The previously reported improvements in fluoride release and activity in acidic environments were not verified for the produced CaF_2 MP. A reproducible version of the CaF_2 NP production protocol is necessary before the nanocomposite membranes described by Estrada can be tested for anti-biofouling activity.

In their current state, the Ag NP nanocomposite ultrafiltration membranes produced in this dissertation are unlikely to achieve any substantial and long-lasting biofouling prevention. UF membrane surfaces are expected to accumulate organic foulants during filtration, including from non-viable bacteria (Guo et al., 2012), making the membrane surface an environment richer in protein than the feed. As filtration proceeds, a decrease in silver available for antibacterial activity may therefore occur. This possibility warrants further study, as it could be one of the main limiting factors in the activity of Ag NP nanocomposite membranes. The dependence on silver leaching for anti-biofouling presents additional limitations. Taurozzi *et al.* demonstrated that, under filtration, a Ag NP nanocomposite ultrafiltration membrane lost anti-biofouling properties due to the displacement of the antibacterial agents from the membrane surface to the permeate (Taurozzi et al., 2008); backwashing, which would bring silver into the membrane surface, was not evaluated. If silver leaching during filtration occurs to the same degree as observed during the 13-day period of membrane incubation, the membranes would quickly become depleted of Ag NP. Long term filtration assays, with media and environmental conditions (temperature and oxygen concentration, for example) similar to the operation conditions of a full-scale membrane system must be undertaken to evaluate the longevity of the membranes. The nature of the silver leachate, whether it is ionic or nanoparticles, must also be evaluated.

5. References

Al-Amoudi, A., & Lovitt, R. W. (2007). Fouling strategies and the cleaning system of NF membranes and factors affecting cleaning efficiency. In *Journal of Membrane Science* (Vol. 303, Issues 1–2, pp. 4–28). Elsevier. https://doi.org/10.1016/j.memsci.2007.06.002

Allgeier, S., Alspach, B., Vickers, J., Alt, S., Cherry, J., Donnelly, M., Hill, C., & Patrick, S. (2005). *Membrane Filtration Guidance Manual* (Issue November). United States Environmental Protection Agency Office.

Badruzzaman, M., Voutchkov, N., Weinrich, L., & Jacangelo, J. G. (2019). Selection of pretreatment technologies for seawater reverse osmosis plants: A review. In *Desalination* (Vol. 449, pp. 78–91). Elsevier B.V. https://doi.org/10.1016/j.desal.2018.10.006

Baker, J. S., & Dudley, L. Y. (1998). Biofouling in membrane systems - a review. *Desalination*, *118*(1–3), 81–89. https://doi.org/10.1016/S0011-9164(98)00091-5

Bala, W. A., Benitha, V. S., Jeyasubramanian, K., Hikku, G. S., Sankar, P., & Kumar, S. V. (2017). Investigation of anti-bacterial activity and cytotoxicity of calcium fluoride nanoparticles. *Journal of Fluorine Chemistry*, *193*, 38–44. https://doi.org/10.1016/j.jfluchem.2016.11.014

Bar-Zeev, E., Berman-Frank, I., Girshevitz, O., & Berman, T. (2012). Revised paradigm of aquatic biofilm formation facilitated by microgel transparent exopolymer particles. *Proceedings of the National Academy of Sciences of the United States of America*, *109*(23), 9119–9124. https://doi.org/10.1073/pnas.1203708109

Bar-Zeev, E., Passow, U., Romero-Vargas Castrillón, S., & Elimelech, M. (2015). Transparent exopolymer particles: From aquatic environments and engineered systems to membrane biofouling. In *Environmental Science and Technology* (Vol. 49, Issue 2, pp. 691–707). American Chemical Society. https://doi.org/10.1021/es5041738

Beisl, S., Monteiro, S., Santos, R., Figueiredo, A. S., Sánchez-Loredo, M. G., Lemos, M. A., Lemos, F., Minhalma, M., & de Pinho, M. N. (2019). Synthesis and bactericide activity of nanofiltration composite membranes – Cellulose acetate/silver nanoparticles and cellulose acetate/silver ion exchanged zeolites. *Water Research*, *149*, 225–231. https://doi.org/10.1016/j.watres.2018.10.096

Bereschenko, L. A., Stams, A. J. M., Euverink, G. J. W., & Van Loosdrecht, M. C. M. (2010). Biofilm formation on reverse osmosis membranes is initiated and dominated by *Sphingomonas* spp. *Applied and Environmental Microbiology*, *76*(8), 2623–2632. https://doi.org/10.1128/AEM.01998-09

Bogler, A., Lin, S., & Bar-Zeev, E. (2017). Biofouling of membrane distillation, forward osmosis and pressure retarded osmosis: Principles, impacts and future directions. In *Journal of Membrane Science* (Vol. 542, pp. 378–398). Elsevier B.V. https://doi.org/10.1016/j.memsci.2017.08.001

Bootz, A., Vogel, V., Schubert, D., & Kreuter, J. (2004). Comparison of scanning electron microscopy, dynamic light scattering and analytical ultracentrifugation for the sizing of poly(butyl cyanoacrylate) nanoparticles. *European Journal of Pharmaceutics and Biopharmaceutics*, *57*(2), 369–375. https://doi.org/10.1016/S0939-6411(03)00193-0

Bratthall, D., Hänsel-Petersson, G., & Sundberg, H. (1996). Reasons for the caries decline: what do the experts believe? *European Journal of Oral Sciences*, *104*(4 (Pt 2)), 416–422. https://doi.org/10.1111/j.1600-0722.1996.tb00104.x

Buzalaf, M. A. R., Pessan, J. P., Honório, H. M., & ten Cate, J. M. (2011). Mechanisms of Action of Fluoride for Caries Control. In *Monographs in Oral Science* (Vol. 22, pp. 97–114). Karger Publishers. https://doi.org/10.1159/000325151

Chernousova, S., & Epple, M. (2013). Silver as antibacterial agent: Ion, nanoparticle, and metal. In *Angewandte Chemie - International Edition* (Vol. 52, Issue 6, pp. 1636–1653). John Wiley & Sons, Ltd. https://doi.org/10.1002/anie.201205923

Choi, O., & Hu, Z. (2008). Size dependent and reactive oxygen species related nanosilver toxicity to

nitrifying bacteria. *Environmental Science and Technology*, *42*(12), 4583–4588. https://doi.org/10.1021/es703238h

Cogan, N. G., Li, J., Badireddy, A. R., & Chellam, S. (2016). Optimal backwashing in dead-end bacterial microfiltration with irreversible attachment mediated by extracellular polymeric substances production. *Journal of Membrane Science*, *520*, 337–344. https://doi.org/10.1016/j.memsci.2016.08.001

Crittenden, J. C., Trussel, R. R., Hand, D. W., Howe, K. J., & Tchobanoglous, G. (2012). Membrane Filtration. In *MWH's Water Treatment: Principles and Design* (Third Edition, pp. 819–902). John Wiley & Sons, Inc. https://doi.org/10.1002/9781118131473.ch12

Cruz, M. C., Ruano, G., Wolf, M., Hecker, D., Castro Vidaurre, E., Schmittgens, R., & Rajal, V. B. (2015). Plasma deposition of silver nanoparticles on ultrafiltration membranes: Antibacterial and anti-biofouling properties. *Chemical Engineering Research and Design*, *94*, 524–537. https://doi.org/10.1016/j.cherd.2014.09.014

Curran, T. M., Buckley, D. H., & Marquis, R. E. (1994). Quasi-irreversible inhibition of enolase of *Streptococcus mutans* by flouride. *FEMS Microbiology Letters*, *119*(3), 283–288. https://doi.org/10.1111/j.1574-6968.1994.tb06902.x

De Leersnyder, I., De Gelder, L., Van Driessche, I., & Vermeir, P. (2018). Influence of growth media components on the antibacterial effect of silver ions on *Bacillus subtilis* in a liquid growth medium. *Scientific Reports*, *8*(1), 1–10. https://doi.org/10.1038/s41598-018-27540-9

de Sousa, M. B., de Pinho, M. N., & dos Santos, P. C. (2014). The role of polysaccharides on the grape must ultrafiltration performance. *Ciencia e Tecnica Vitivinicola*, *29*(1), 16–27. https://doi.org/10.1051/ctv/20142901016

Decarolis, J., Hong, S., & Taylor, J. (2001). Fouling behavior of a pilot scale inside-out hollow fiber UF membrane during dead-end filtration of tertiary wastewater. *Journal of Membrane Science*, *191*(1–2), 165–178. https://doi.org/10.1016/S0376-7388(01)00455-0

Duan, L., Zhao, Q., Liu, J., & Zhang, Y. (2015). Antibacterial behavior of halloysite nanotubes decorated with copper nanoparticles in a novel mixed matrix membrane for water purification. *Environmental Science: Water Research and Technology*, *1*(6), 874–881. https://doi.org/10.1039/c5ew00140d

Eckhardt, S., Brunetto, P. S., Gagnon, J., Priebe, M., Giese, B., & Fromm, K. M. (2013). Nanobio silver: Its interactions with peptides and bacteria, and its uses in medicine. In *Chemical Reviews* (Vol. 113, Issue 7, pp. 4708–4754). American Chemical Society. https://doi.org/10.1021/cr300288v

El Badawy, A. M., Silva, R. G., Morris, B., Scheckel, K. G., Suidan, M. T., & Tolaymat, T. M. (2011). Surface charge-dependent toxicity of silver nanoparticles. *Environmental Science and Technology*, *45*(1), 283–287. https://doi.org/10.1021/es1034188

Esfahani, M. R., Aktij, S. A., Dabaghian, Z., Firouzjaei, M. D., Rahimpour, A., Eke, J., Escobar, I. C., Abolhassani, M., Greenlee, L. F., Esfahani, A. R., Sadmani, A., & Koutahzadeh, N. (2019). Nanocomposite membranes for water separation and purification: Fabrication, modification, and applications. In *Separation and Purification Technology* (Vol. 213, pp. 465–499). Elsevier B.V. https://doi.org/10.1016/j.seppur.2018.12.050

Estrada, A. M. (2017). *Efecto de la modificación de membranas asimétricas de acetato de celulosa con partículas ultrafinas de fluoruro de calcio*. Universidad Autónoma de San Luis Potosí.

Fane, A. G., Wang, R., & Hu, M. X. (2015). Synthetic membranes for water purification: Status and future. *Angewandte Chemie - International Edition*, *54*(11), 3368–3386. https://doi.org/10.1002/anie.201409783

Feng, Q. L., Wu, J., Chen, G. Q., Cui, F. Z., Kim, T. N., & Kim, J. O. (2000). A mechanistic study of the antibacterial effect of silver ions on Escherichia coli and Staphylococcus aureus. *Journal of*

Biomedical Materials Research, *52*(4), 662–668. https://doi.org/10.1002/1097-4636(20001215)52:4<662::AID-JBM10>3.0.CO;2-3

Figueiredo, A. S. (2016). *Asymmetric nanocomposite cellulose acetate / silver ultrafiltration membranes – Permeation performance and antibacterial effect*. University of Lisbon - Instituto Superior Técnico.

Figueiredo, A. S., Sánchez-Loredo, M. G., Maurício, A., Pereira, M. F. C., Minhalma, M., & de Pinho, M. N. (2015). Tailoring of structures and permeation properties of asymmetric nanocomposite cellulose acetate/silver membranes. *Journal of Applied Polymer Science*, *132*(21). https://doi.org/10.1002/app.41796

Gao, W., Liang, H., Ma, J., Han, M., Chen, Z. lin, Han, Z. shuang, & Li, G. bai. (2011). Membrane fouling control in ultrafiltration technology for drinking water production: A review. In *Desalination* (Vol. 272, Issues 1–3, pp. 1–8). Elsevier. https://doi.org/10.1016/j.desal.2011.01.051

Gordon, O., Slenters, T. V., Brunetto, P. S., Villaruz, A. E., Sturdevant, D. E., Otto, M., Landmann, R., & Fromm, K. M. (2010). Silver coordination polymers for prevention of implant infection: Thiol interaction, impact on respiratory chain enzymes, and hydroxyl radical induction. *Antimicrobial Agents and Chemotherapy*, *54*(10), 4208–4218. https://doi.org/10.1128/AAC.01830-09

Guo, W., Ngo, H. H., & Li, J. (2012). A mini-review on membrane fouling. *Bioresource Technology*, *122*, 27–34. https://doi.org/10.1016/j.biortech.2012.04.089

Gupta, A., Maynes, M., & Silver, S. (1998). Effects of halides on plasmid-mediated silver resistance in Escherichia coli. *Applied and Environmental Microbiology*, *64*(12), 5042–5045. https://doi.org/10.1128/aem.64.12.5042-5045.1998

Gutknecht, J., & Walter, A. (1981). Hydrofluoric and nitric acid transport through lipid bilayer membranes. *BBA - Biomembranes*, *644*(1), 153–156. https://doi.org/10.1016/0005-2736(81)90071-7

Harrison, P. T. C. (2005). Fluoride in water: A UK perspective. In *Journal of Fluorine Chemistry* (Vol. 126, Issues 11–12, pp. 1448–1456). Elsevier. https://doi.org/10.1016/j.jfluchem.2005.09.009

Helmlinger, J., Sengstock, C., Groß-Heitfeld, C., Mayer, C., Schildhauer, T. A., Köller, M., & Epple, M. (2016). Silver nanoparticles with different size and shape: Equal cytotoxicity, but different antibacterial effects. *RSC Advances*, *6*(22), 18490–18501. https://doi.org/10.1039/c5ra27836h

Holt, K. B., & Bard, A. J. (2005). Interaction of silver(I) ions with the respiratory chain of *Escherichia coli*: An electrochemical and scanning electrochemical microscopy study of the antimicrobial mechanism of micromolar Ag. *Biochemistry*, *44*(39), 13214–13223. https://doi.org/10.1021/bi0508542

Huang, H., Schwab, K., & Jacangelo, J. G. (2009). Pretreatment for low pressure membranes in water treatment: A review. In *Environmental Science and Technology* (Vol. 43, Issue 9, pp. 3011–3019). American Chemical Society. https://doi.org/10.1021/es802473r

Inaba, T., Hori, T., Aizawa, H., Ogata, A., & Habe, H. (2017). Architecture, component, and microbiome of biofilm involved in the fouling of membrane bioreactors. *Npj Biofilms and Microbiomes*, *3*(1), 0–1. https://doi.org/10.1038/s41522-016-0010-1

Ji, C., Stockbridge, R. B., & Miller, C. (2014). Bacterial fluoride resistance, Fluc channels, and the weak acid accumulation effect. *Journal of General Physiology*, *144*(3), 257–261. https://doi.org/10.1085/jgp.201411243

Kesting, R. E., & Menefee, A. (1969). The role of formamide in the preparation of cellulose acetate membranes by the phase inversion process. *Kolloid-Zeitschrift & Zeitschrift Für Polymere*, *230*(2), 341–346. https://doi.org/10.1007/BF01520608

Khan, M. T., Manes, C. L. de O., Aubry, C., & Croué, J. P. (2013). Source water quality shaping different fouling scenarios in a full-scale desalination plant at the Red Sea. *Water Research*, *47*(2), 558–568. https://doi.org/10.1016/j.watres.2012.10.017

Kimura, K., Hane, Y., Watanabe, Y., Amy, G., & Ohkuma, N. (2004). Irreversible membrane fouling during ultrafiltration of surface water. *Water Research*, *38*(14–15), 3431–3441. https://doi.org/10.1016/j.watres.2004.05.007

Klasen, H. J. (2000a). A historical review of the use of silver in the treatment of burns. II. Renewed interest for silver. In *Burns* (Vol. 26, Issue 2, pp. 131–138). Elsevier Ltd. https://doi.org/10.1016/S0305-4179(99)00116-3

Klasen, H. J. (2000b). Historical review of the use of silver in the treatment of burns. I. Early uses. In *Burns* (Vol. 26, Issue 2, pp. 117–130). Elsevier Ltd. https://doi.org/10.1016/S0305-4179(99)00108-4

Kochkodan, V., & Hilal, N. (2015). A comprehensive review on surface modified polymer membranes for biofouling mitigation. In *Desalination* (Vol. 356, pp. 187–207). Elsevier. https://doi.org/10.1016/j.desal.2014.09.015

Koczkur, K. M., Mourdikoudis, S., Polavarapu, L., & Skrabalak, S. E. (2015). Polyvinylpyrrolidone (PVP) in nanoparticle synthesis. *Dalton Transactions*, *44*(41), 17883–17905. https://doi.org/10.1039/c5dt02964c

Koros, W. J., Ma, Y. H., & Shimidzu, T. (1996). Terminology for membranes and membrane processes (IUPAC Recommendations 1996). *Pure and Applied Chemistry*, *68*(7), 1479–1489. https://doi.org/10.1351/pac199668071479

Kulshrestha, S., Khan, S., Hasan, S., Khan, M. E., Misba, L., & Khan, A. U. (2016). Calcium fluoride nanoparticles induced suppression of *Streptococcus mutans* biofilm: an in vitro and in vivo approach. *Applied Microbiology and Biotechnology*, *100*(4), 1901–1914. https://doi.org/10.1007/s00253-015-7154-4

Kunst, B., & Sourirajan, S. (1974). An approach to the development of cellulose acetate ultrafiltration membranes. *Journal of Applied Polymer Science*, *18*(11), 3423–3434. https://doi.org/10.1002/app.1974.070181121

Lall, U., Josset, L., & Russo, T. (2020). A Snapshot of the World's Groundwater Challenges. *Annual Review of Environment and Resources*, *45*(1), 171–194. https://doi.org/10.1146/annurev-environ-102017-025800

Landsman, M. R., Sujanani, R., Brodfuehrer, S. H., Cooper, C. M., Darr, A. G., Davis, R. J., Kim, K., Kum, S., Nalley, L. K., Nomaan, S. M., Oden, C. P., Paspureddi, A., Reimund, K. K., Rowles, L. S., Yeo, S., Lawler, D. F., Freeman, B. D., & Katz, L. E. (2020). Water Treatment: Are Membranes the Panacea? *Annual Review of Chemical and Biomolecular Engineering*, *11*(1), 559–585. https://doi.org/10.1146/annurev-chembioeng-111919-091940

Li, W. R., Xie, X. B., Shi, Q. S., Zeng, H. Y., Ou-Yang, Y. S., & Chen, Y. Ben. (2010). Antibacterial activity and mechanism of silver nanoparticles on Escherichia coli. *Applied Microbiology and Biotechnology*, *85*(4), 1115–1122. https://doi.org/10.1007/s00253-009-2159-5

Liao, Y., Brandt, B. W., Li, J., Crielaard, W., Van Loveren, C., & Deng, D. M. (2017). Fluoride resistance in *Streptococcus mutans* : a mini review. *Journal of Oral Microbiology*, *9*(1), 1344509. https://doi.org/10.1080/20002297.2017.1344509

Liau, S. Y., Read, D. C., Pugh, W. J., Furr, J. R., & Russell, A. D. (1997). Interaction of silver nitrate with readily identifiable groups: Relationship to the antibacterial action of silver ions. *Letters in Applied Microbiology*, *25*(4), 279–283. https://doi.org/10.1046/j.1472-765X.1997.00219.x

Lok, C. N., Ho, C. M., Chen, R., He, Q. Y., Yu, W. Y., Sun, H., Tam, P. K. H., Chiu, J. F., & Che, C. M. (2007). Silver nanoparticles: Partial oxidation and antibacterial activities. *Journal of Biological Inorganic Chemistry*, *12*(4), 527–534. https://doi.org/10.1007/s00775-007-0208-z

Madsen, H. T. (2014). Membrane Filtration in Water Treatment - Removal of Micropollutants. In *Chemistry of Advanced Environmental Purification Processes of Water: Fundamentals and Applications*. https://doi.org/10.1016/B978-0-444-53178-0.00006-7

Mansouri, J., Harrisson, S., & Chen, V. (2010). Strategies for controlling biofouling in membrane filtration systems: Challenges and opportunities. *Journal of Materials Chemistry*, *20*(22), 4567–4586. https://doi.org/10.1039/b926440j

Marambio-Jones, C., & Hoek, E. M. V. (2010). A review of the antibacterial effects of silver nanomaterials and potential implications for human health and the environment. In *Journal of Nanoparticle Research* (Vol. 12, Issue 5, pp. 1531–1551). Springer. https://doi.org/10.1007/s11051-010-9900-y

Marquis, R. E. (1990). Diminished acid tolerance of plaque bacteria caused by fluoride. *Journal of Dental Research*, *69*(SPEC. ISS. FEB.), 672–675. https://doi.org/10.1177/00220345900690s130

Marquis, R. E., Clock, S. A., & Mota-Meira, M. (2003). Fluoride and organic weak acids as modulators of microbial physiology. *FEMS Microbiology Reviews*, *26*(5), 493–510. https://doi.org/10.1111/j.1574-6976.2003.tb00627.x

Matin, A., Khan, Z., Zaidi, S. M. J., & Boyce, M. C. (2011). Biofouling in reverse osmosis membranes for seawater desalination: Phenomena and prevention. In *Desalination* (Vol. 281, Issue 1, pp. 1–16). Elsevier. https://doi.org/10.1016/j.desal.2011.06.063

McCarthy, A. A., Walsh, P. K., & Foley, G. (2002). Experimental techniques for quantifying the cake mass, the cake and membrane resistances and the specific cake resistance during crossflow filtration of microbial suspensions. *Journal of Membrane Science*, *201*(1–2), 31–45. https://doi.org/10.1016/S0376-7388(01)00691-3

Medici, S., Peana, M., Nurchi, V. M., & Zoroddu, M. A. (2019). Medical Uses of Silver: History, Myths, and Scientific Evidence. In *Journal of Medicinal Chemistry* (Vol. 62, Issue 13, pp. 5923–5943). American Chemical Society. https://doi.org/10.1021/acs.jmedchem.8b01439

Mickols, W. E. (2012). Aromatic Poly(amides) for Reverse Osmosis. In *Polymer Science: A Comprehensive Reference, 10 Volume Set* (Vol. 10). Elsevier B.V. https://doi.org/10.1016/B978-0-444-53349-4.00295-8

Mirzajani, F., Ghassempour, A., Aliahmadi, A., & Esmaeili, M. A. (2011). Antibacterial effect of silver nanoparticles on *Staphylococcus aureus*. *Research in Microbiology*, *162*(5), 542–549. https://doi.org/10.1016/j.resmic.2011.04.009

Miura, Y., Watanabe, Y., & Okabe, S. (2007). Membrane biofouling in pilot-scale membrane bioreactors (MBRs) treating municipal wastewater: Impact of biofilm formation. *Environmental Science and Technology*, *41*(2), 632–638. https://doi.org/10.1021/es0615371

Morones, J. R., Elechiguerra, J. L., Camacho, A., Holt, K., Kouri, J. B., Ramírez, J. T., & Yacaman, M. J. (2005). The bactericidal effect of silver nanoparticles. *Nanotechnology*, *16*(10), 2346–2353. https://doi.org/10.1088/0957-4484/16/10/059

Nagaraj, V., Skillman, L., Ho, G., Li, D., & Gofton, A. (2017). Characterisation and comparison of bacterial communities on reverse osmosis membranes of a full-scale desalination plant by bacterial 16S rRNA gene metabarcoding. *Npj Biofilms and Microbiomes*, *3*(1), 1–13. https://doi.org/10.1038/s41522-017-0021-6

National Center for Biotechnology Information. (2020). *PubChem Compound Summary for CID 84512, Calcium fluoride.* https://pubchem.ncbi.nlm.nih.gov/compound/Calcium-fluoride

Ng, L. Y., Mohammad, A. W., Leo, C. P., & Hilal, N. (2013). Polymeric membranes incorporated with metal/metal oxide nanoparticles: A comprehensive review. In *Desalination* (Vol. 308, pp. 15–33). Elsevier. https://doi.org/10.1016/j.desal.2010.11.033

Nowack, B., Krug, H. F., & Height, M. (2011). 120 years of nanosilver history: Implications for policy makers. *Environmental Science and Technology*, *45*(4), 1177–1183.

https://doi.org/10.1021/es103316q

Panáček, A., Kvítek, L., Prucek, R., Kolář, M., Večeřová, R., Pizúrová, N., Sharma, V. K., Nevěčná, T., & Zbořil, R. (2006). Silver colloid nanoparticles: Synthesis, characterization, and their antibacterial activity. *Journal of Physical Chemistry B*, *110*(33), 16248–16253. https://doi.org/10.1021/jp063826h

Park, H.-J., Yeon Kim, J., Kim, J., Lee, J.-H., Hahn, J.-S., Bock Gu, M., & Yoon, J. (2008). Silver-ion-mediated reactive oxygen species generation affecting bactericidal activity. *Water Research*, *43*, 1027–1032. https://doi.org/10.1016/j.watres.2008.12.002

Park, H. B., Freeman, B. D., Zhang, Z. B., Sankir, M., & McGrath, J. E. (2008). Highly chlorine-tolerant polymers for desalination. *Angewandte Chemie - International Edition*, *47*(32), 6019–6024. https://doi.org/10.1002/anie.200800454

Petersen, R. J. (1993). Composite reverse osmosis and nanofiltration membranes. In *Journal of Membrane Science* (Vol. 83, Issue 1, pp. 81–150). Elsevier. https://doi.org/10.1016/0376-7388(93)80014-O

Plappally, A. K., & Lienhard V, J. H. (2012). Energy requirements for water production, treatment, end use, reclamation, and disposal. In *Renewable and Sustainable Energy Reviews* (Vol. 16, Issue 7, pp. 4818–4848). Pergamon. https://doi.org/10.1016/j.rser.2012.05.022

Polanska, M., Huysman, K., & Van Keer, C. (2005). Investigation of assimilable organic carbon (AOC) in flemish drinking water. *Water Research*, *39*(11), 2259–2266. https://doi.org/10.1016/j.watres.2005.04.015

Quinteros, M. A., Cano Aristizábal, V., Dalmasso, P. R., Paraje, M. G., & Páez, P. L. (2016). Oxidative stress generation of silver nanoparticles in three bacterial genera and its relationship with the antimicrobial activity. *Toxicology in Vitro*, *36*, 216–223. https://doi.org/10.1016/j.tiv.2016.08.007

Ratte, H. T. (1999). Bioaccumulation and toxicity of silver compounds: A review. *Environmental Toxicology and Chemistry*, *18*(1), 89–108. https://doi.org/10.1002/etc.5620180112

Sarkar, A., Kapoor, S., & Mukherjee, T. (2005). Preparation, characterization, and surface modification of silver nanoparticles in formamide. *Journal of Physical Chemistry B*, *109*(16), 7698–7704. https://doi.org/10.1021/jp044201r

Saurí, D. (2013). Water Conservation: Theory and Evidence in Urban Areas of the Developed World. *Annual Review of Environment and Resources*, *38*(1), 227–248. https://doi.org/10.1146/annurev-environ-013113-142651

Semiat, R. (2008). Energy issues in desalination processes. In *Environmental Science and Technology* (Vol. 42, Issue 22, pp. 8193–8201). American Chemical Society. https://doi.org/10.1021/es801330u

Sheng, Z., & Liu, Y. (2011). Effects of silver nanoparticles on wastewater biofilms. *Water Research*, *45*(18), 6039–6050. https://doi.org/10.1016/j.watres.2011.08.065

Shi, X., Tal, G., Hankins, N. P., & Gitis, V. (2014). Fouling and cleaning of ultrafiltration membranes: A review. In *Journal of Water Process Engineering* (Vol. 1, pp. 121–138). Elsevier Ltd. https://doi.org/10.1016/j.jwpe.2014.04.003

Solomon, S. D., Bahadory, M., Jeyarajasingam, A. V., Rutkowsky, S. A., Boritz, C., & Mulfinger, L. (2007). Synthesis and study of silver nanoparticles. *Journal of Chemical Education*, *84*(2), 322–325. https://doi.org/10.1021/ed084p322

Sonawane, S. H., Terrien, A., Figueiredo, A. S., Clara Gonçalves, M., & De Pinho, M. N. (2017). The role of silver nanoparticles on mixed matrix Ag/cellulose acetate asymmetric membranes. *Polymer Composites*, *38*(1), 32–39. https://doi.org/10.1002/pc.23557

Sondi, I., & Salopek-Sondi, B. (2004). Silver nanoparticles as antimicrobial agent: A case study on *E.*

coli as a model for Gram-negative bacteria. *Journal of Colloid and Interface Science*, *275*(1), 177–182. https://doi.org/10.1016/j.jcis.2004.02.012

Sprick, C., Chede, S., Oyanedel-Craver, V., & Escobar, I. C. (2018). Bio-inspired immobilization of casein-coated silver nanoparticles on cellulose acetate membranes for biofouling control. *Journal of Environmental Chemical Engineering*, *6*(2), 2480–2491. https://doi.org/10.1016/j.jece.2018.03.044

Sturr, M. G., & Marquis, R. E. (1990). Inhibition of proton-translocating ATPases of *Streptococcus mutans* and *Lactobacillus casei* by fluoride and aluminum. *Archives of Microbiology*, *155*(1), 22–27. https://doi.org/10.1007/BF00291269

Taurozzi, J. S., Arul, H., Bosak, V. Z., Burban, A. F., Voice, T. C., Bruening, M. L., & Tarabara, V. V. (2008). Effect of filler incorporation route on the properties of polysulfone-silver nanocomposite membranes of different porosities. *Journal of Membrane Science*, *325*(1), 58–68. https://doi.org/10.1016/j.memsci.2008.07.010

Tejamaya, M., Römer, I., Merrifield, R. C., & Lead, J. R. (2012). Stability of citrate, PVP, and PEG coated silver nanoparticles in ecotoxicology media. *Environmental Science and Technology*, *46*(13), 7011–7017. https://doi.org/10.1021/es2038596

Tran, T., Bolto, B., Gray, S., Hoang, M., & Ostarcevic, E. (2007). An autopsy study of a fouled reverse osmosis membrane element used in a brackish water treatment plant. *Water Research*, *41*(17), 3915–3923. https://doi.org/10.1016/j.watres.2007.06.008

Vert, M., Doi, Y., Hellwich, K. H., Hess, M., Hodge, P., Kubisa, P., Rinaudo, M., & Schué, F. (2012). Terminology for biorelated polymers and applications (IUPAC recommendations 2012). *Pure and Applied Chemistry*, *84*(2), 377–410. https://doi.org/10.1351/pac-rec-10-12-04

Vogel, V., Gohy, J.-F., Lohmeijer, B. G. G., Van Den Broek, J. A., Haase, W., Schubert, U. S., & Schubert, D. (2003). Metallo-supramolecular micelles: Studies by analytical ultracentrifugation and electron microscopy. *Journal of Polymer Science Part A: Polymer Chemistry*, *41*(20), 3159–3168. https://doi.org/10.1002/pola.10902

Wasiak, J., Cleland, H., Campbell, F., & Spinks, A. (2013). Dressings for superficial and partial thickness burns. In *Cochrane Database of Systematic Reviews* (Vol. 2013, Issue 3). John Wiley and Sons Ltd. https://doi.org/10.1002/14651858.CD002106.pub4

Whitford, G. M., Schuster, G. S., Pashley, D. H., & Venkateswarlu, P. (1977). Fluoride uptake by *Streptococcus mutans* 6715. *Infection and Immunity*, *18*(3), 680–687.

Xiu, Z. M., Ma, J., & Alvarez, P. J. J. (2011). Differential effect of common ligands and molecular oxygen on antimicrobial activity of silver nanoparticles versus silver ions. *Environmental Science and Technology*, *45*(20), 9003–9008. https://doi.org/10.1021/es201918f

Xiu, Z. M., Zhang, Q. B., Puppala, H. L., Colvin, V. L., & Alvarez, P. J. J. (2012). Negligible particle-specific antibacterial activity of silver nanoparticles. *Nano Letters*, *12*(8), 4271–4275. https://doi.org/10.1021/nl301934w

Xu, H. H. K., Moreau, J. L., Sun, L., & Chow, L. C. (2008). Strength and fluoride release characteristics of a calcium fluoride based dental nanocomposite. *Biomaterials*, *29*(32), 4261–4267. https://doi.org/10.1016/j.biomaterials.2008.07.037

Xu, H. H. K., Moreau, J. L., Sun, L., & Chow, L. C. (2010). Novel CaF2 nanocomposite with high strength and fluoride ion release. *Journal of Dental Research*, *89*(7), 739–745. https://doi.org/10.1177/0022034510364490

Xu, X.-H. N., Brownlow, W. J., Kyriacou, S. V, Wan, Q., & Viola, J. J. (2004). *Real-Time Probing of Membrane Transport in Living Microbial Cells Using Single Nanoparticle Optics and Living Cell Imaging*. https://doi.org/10.1021/bi036231a

Yamamura, H., Kimura, K., & Watanabe, Y. (2007). Mechanism involved in the evolution of physically irreversible fouling in microfiltration and ultrafiltration membranes used for drinking

water treatment. *Environmental Science and Technology*, *41*(19), 6789–6794. https://doi.org/10.1021/es0629054

Yang, Y., & Alvarez, P. J. J. (2015). Sublethal Concentrations of Silver Nanoparticles Stimulate Biofilm Development. *Environmental Science and Technology Letters*, *2*(8), 221–226. https://doi.org/10.1021/acs.estlett.5b00159

Zhang, R., Liu, Y., He, M., Su, Y., Zhao, X., Elimelech, M., & Jiang, Z. (2016). Antifouling membranes for sustainable water purification: Strategies and mechanisms. In *Chemical Society Reviews* (Vol. 45, Issue 21, pp. 5888–5924). Royal Society of Chemistry. https://doi.org/10.1039/c5cs00579e

Zodrow, K., Brunet, L., Mahendra, S., Li, D., Zhang, A., Li, Q., & Alvarez, P. J. J. (2009). Polysulfone ultrafiltration membranes impregnated with silver nanoparticles show improved biofouling resistance and virus removal. *Water Research*, *43*(3), 715–723. https://doi.org/10.1016/j.watres.2008.11.014

Appendixes

Appendix 1: Culture media composition.

- Tryptone bile x-glucoronate agar (Biokar Diagnostics), per 1 L: 20.0 g tryptone; 1.5 g bile salts; 0.075 g 5-bromo-4-chloro-3-indolyl β-D-glucuronate; 9.0 g agar.
- Tryticase soy agar (Biokar Diagnostics), per 1 L: 15.0 g tryptone; 5.0 g papain-digested soy peptone; 5.0 g sodium chloride; 15.0 g agar.
- Slanetz-Bartley medium (Oxoid), per 1 L: 20.0 g tryptone; 5.0 g yeast extract; 2.0 g glucose; 4.0 g di-potassium hydrogen phosphate; 0.4 g sodium azide; 0.1 g tetrazolium chloride; 10.0 g agar.
- Bile esculin agar (Biokar Diagnostics), per 1 L: 17.0 g tryptone; 3.0 g meat peptone; 5.0 g yeast extract; 10.0 g bile salts; 5.0 g sodium chloride; 1.0 g esculin; 0.50 g ammonium ferric citrate; 0.15 g sodium azide; 13.0 g agar.
- Chapman – mannitol salt agar (Biogerm), per 1 L: 1.0 g beef extract; 5.0 g pancreatic digest of casein; 5.0 g peptic digest of animal tissue; 75.0 g sodium chloride; 10.0 g d-mannitol; 0.025 g phenol red; 15.0 g agar.
- Nutrient agar (Biokar Diagnostics), per 1 L: 5.0 g tryptone; 1.0 g meat peptone; 2.0 g yeast extract; 5.0 g sodium chloride; 12.0 g agar.
- Triple sugar iron agar (BD), per 1 L: 10.0 g pancreatic digest of casein; 10.0 g meat peptone; 5.0 g sodium chloride; 10.0 g lactose; 10.0 g sucrose; 1.0 g glucose; 0.2 g ferrous ammonium sulfate; 0.2 g sodium thiosulfate; 0.025 g phenol red; 13.0 g agar.
- CN agar (Biogerm), per 1 L: 16.0 g gelatin peptone; 10.0 g casein hydrolysate; 10.0 g potassium sulphate; 1.4 g magnesium chloride; 0.20 g cetrimide; 0.015g sodium nalidixate; 11.0 g agar.
- Tryptic soy broth (BD), per 1 L: 17.0 g tryptone; 3.0 g soytone; 2.5 g glucose; 5.0 g sodium chloride; 2.5 g dipotassium phosphate.
- Maximum recovery diluent (BD), per 1 L: 1.0 g peptone; 8.5 g sodium chloride.

Appendix 2: Calcium fluoride nanoparticle synthesis

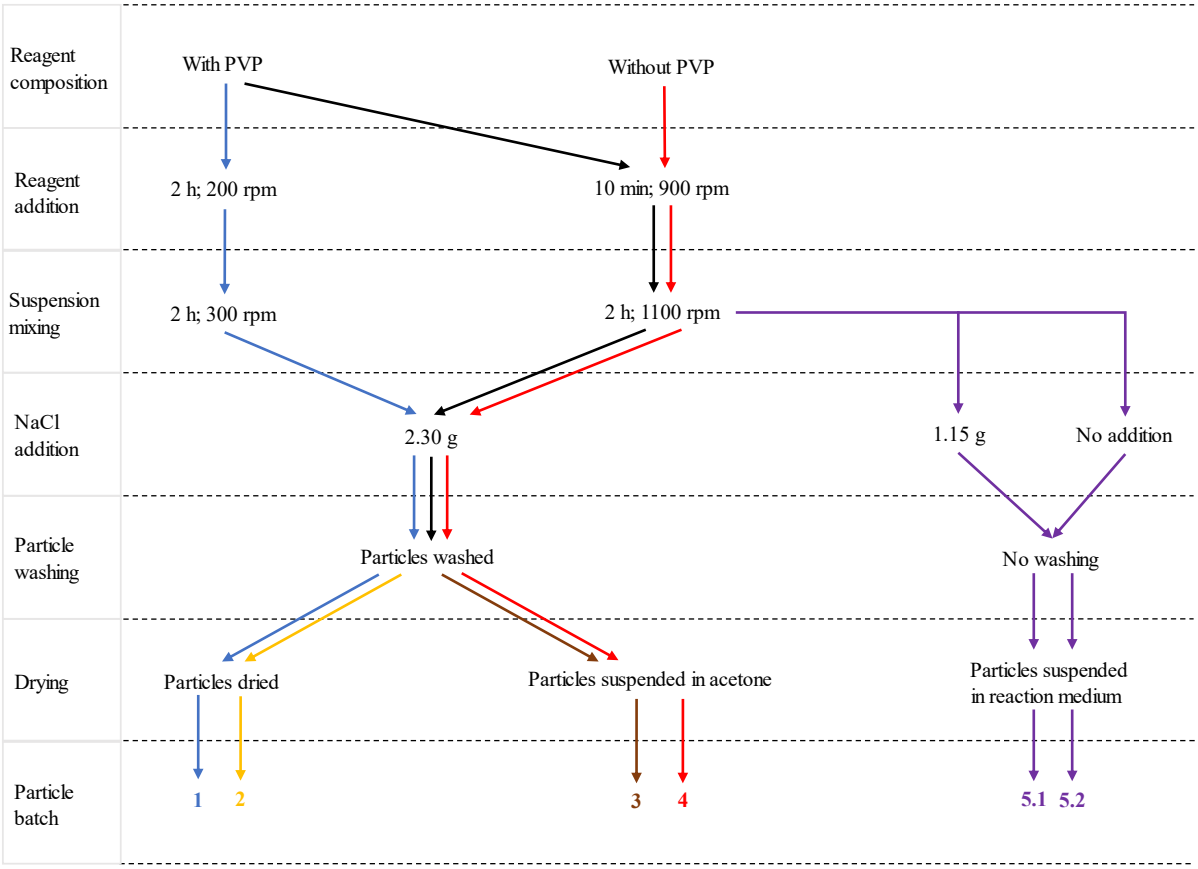

Figure A2.1 – Schematic representation of the differences in synthesis between CaF_2 particle batches. Black arrows represent steps common to multiple batches; blue arrows/numbers represent the 1st batch; yellow arrows/numbers represent the 2nd batch; brown arrows/numbers represent the 3rd batch; red arrows/numbers represent the represent the 4th batch; purple arrows/numbers represent the 5th batch.

Appendix 3: CELFA P-28 calibration plots

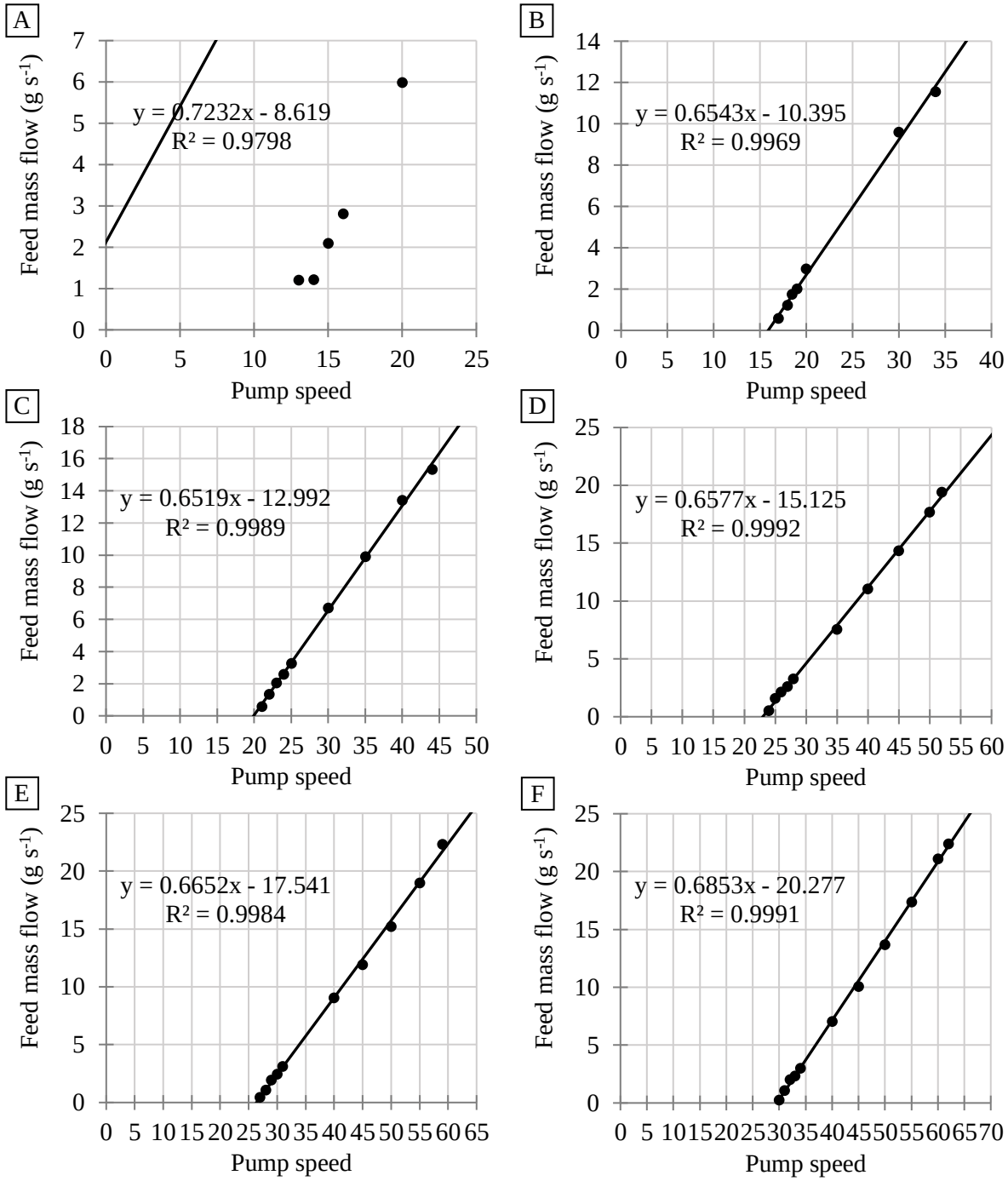

Figure A3.1 – CELFA P-28 calibration plots. A) 0.5 bar; B) 1 bar; C) 1.5 bar; D) 2 bar; E) 2.5 bar; F) 3 bar.

Appendix 4: PEG concentration calibration plots

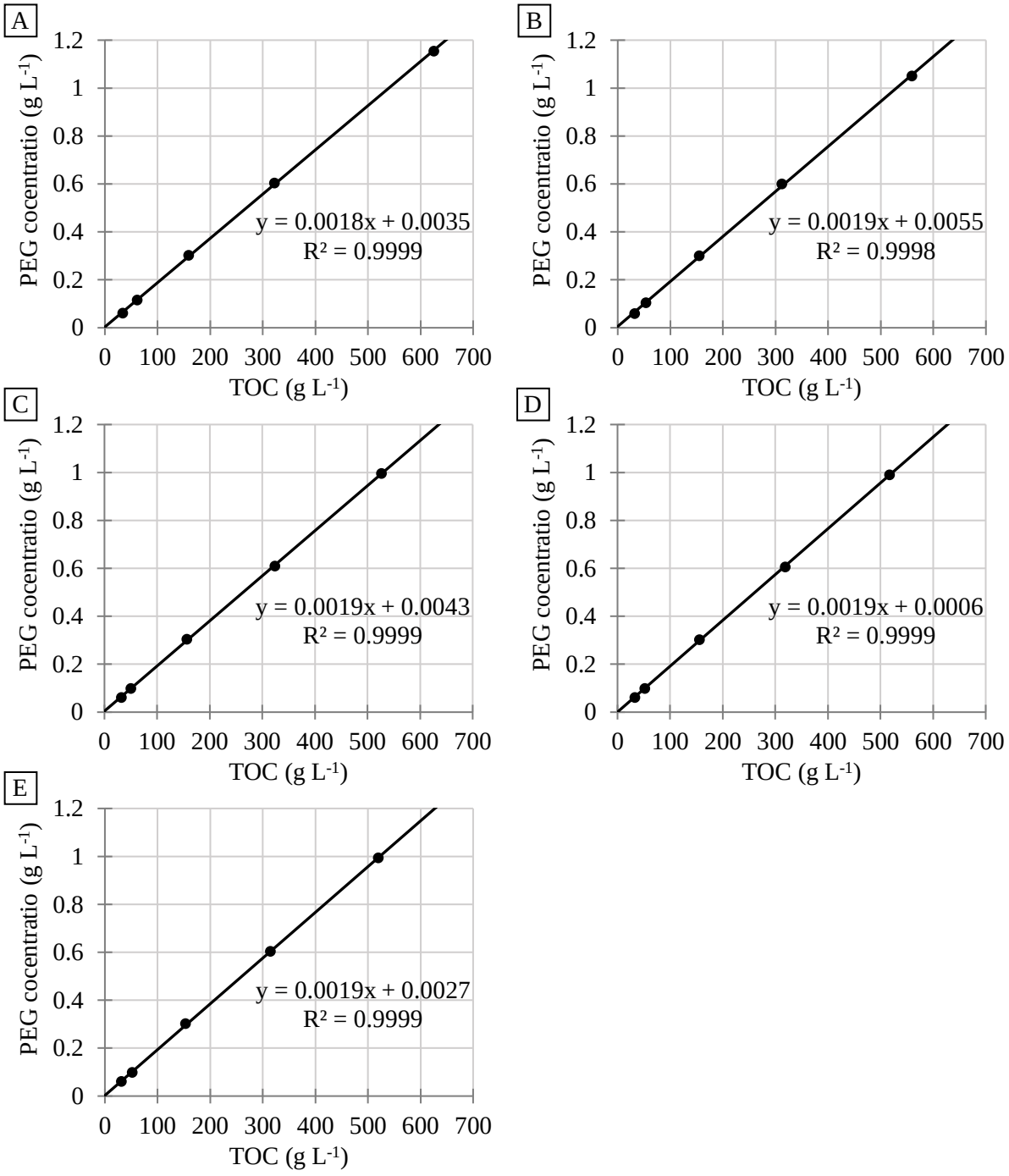

Figure A4.1 – PEG concentration calibration plots. A) PEG 1000; B) PEG 3000; C) PEG 6000; D) PEG 10000; E) PEG 35000.

Appendix 5: Salt rejection coefficient

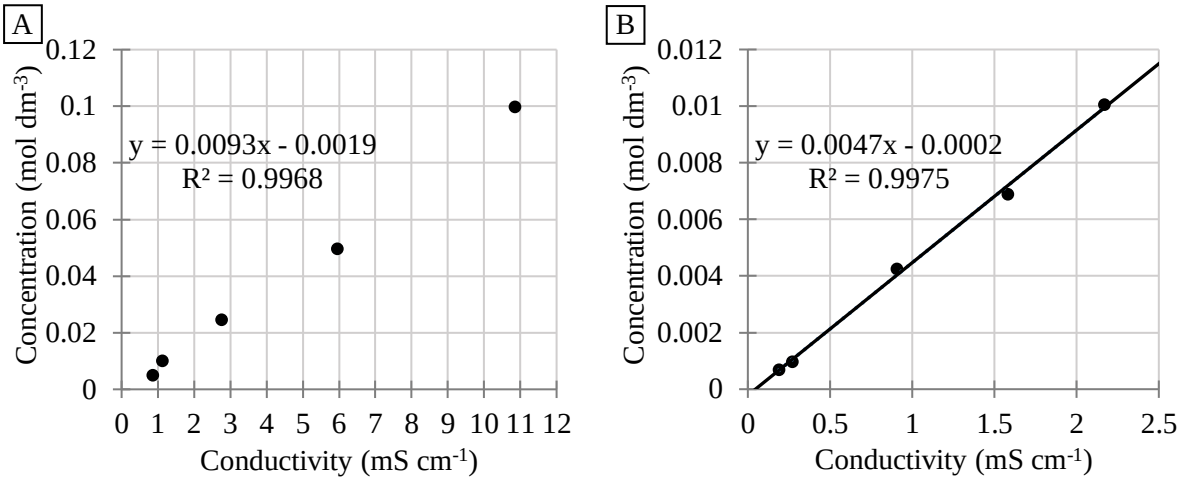

Figure A5.1 – Salt concentration calibration plots. A) NaCl; B) Na_2SO_4.

Table A5.1 – Salt rejection coefficients.

Membrane	CA400-30	CA400-30 Ag 0.1	CA400-30 Ag 0.4
NaCl	2.34%	3.59%	7.19%
Na_2SO_4	1.52%	1.60%	3.22%

Appendix 6: PEG rejection coefficients

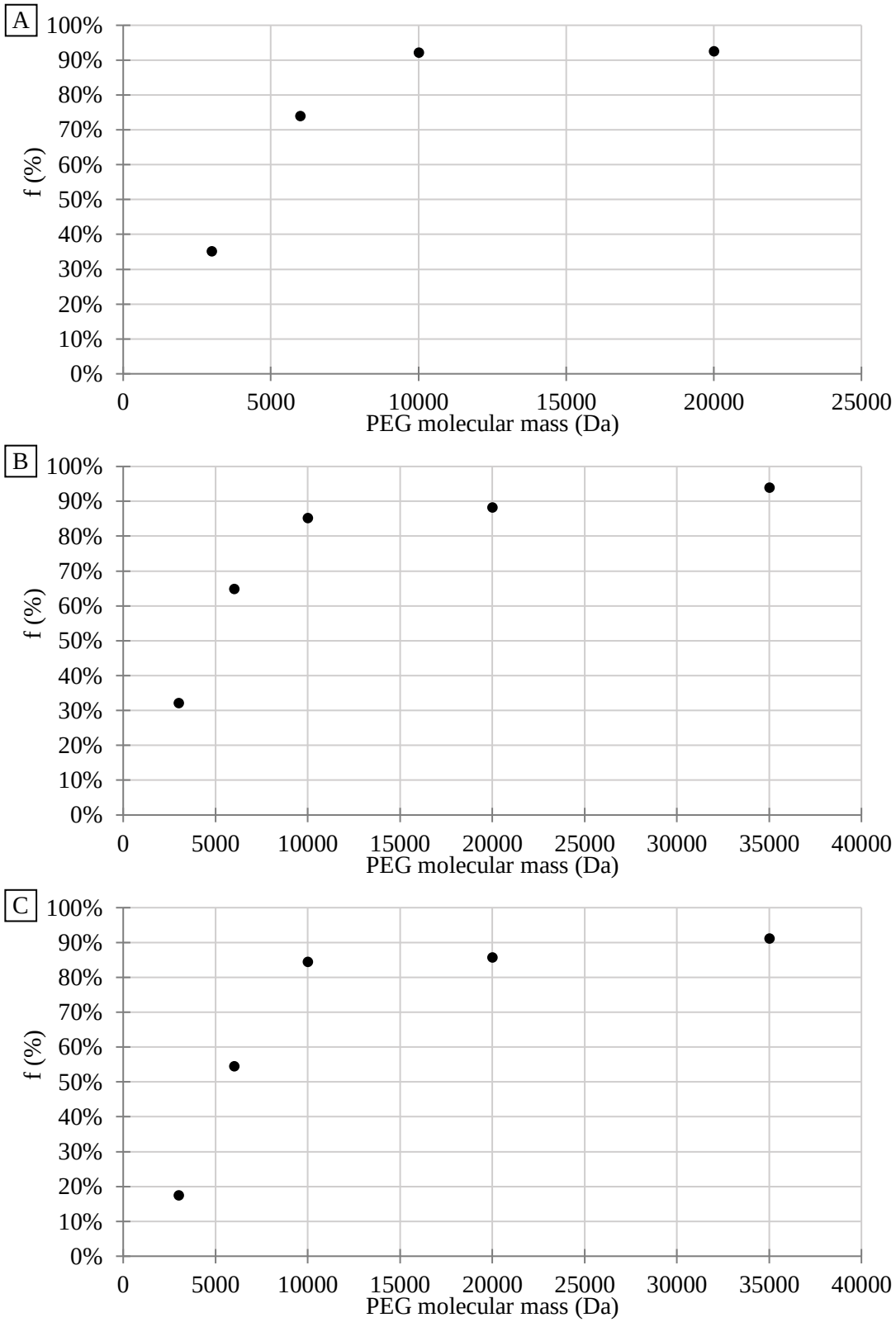

Figure A6.1 – Membrane rejection coefficients for PEG with different molecular mass. A) CA400-30; B) CA400-30 Ag 0.1; C) CA400-30 Ag 0.4.